LYMPH NODE VASCULAR PLASTICITY DURING HERPES SIMPLEX VIRUS TYPE II INFECTION

by

Stephanie L. Sellers

B.Sc., University of Northern British Columbia, 2008

THESIS SUBMITTED IN PARTIAL FULFILLMENT OF
THE REQUIREMENTS FOR THE DEGREE OF
MASTER OF SCIENCE
IN
INTERDISCIPLINARY STUDIES

UNIVERSITY OF NORTHERN BRITISH COLUMBIA

2011

Library and Archives Canada

Published Heritage Branch

395 Wellington Street
Ottawa ON K1A 0N4
Canada

Bibliothèque et Archives Canada

Direction du Patrimoine de l'édition

395, rue Wellington
Ottawa ON K1A 0N4
Canada

Your file Votre référence
ISBN: 978-0-494-87593-3

Our file Notre référence
ISBN: 978-0-494-87593-3

ABSTRACT

Lymph node (LN) blood supply has long been thought to be integral to the immune response. Recently, the phenomenon of remodeling of the LN feed arteriole during viral infection was demonstrated as a key component of induction of an effective adaptive immune response. Here, the data presented show that during infection the LN feed arteriole is capable of non-pathogenic, reversible, outward remodeling peaking seven days post-immunization before returning to pre-infection size. Using pharmacological blockade and genetic ablation models, the remodeling process is demonstrated to be dependent upon the presence of $CD4^+$ T cells in the LN, the expression of endothelial nitric oxide synthase (eNOS), tumor necrosis factor alpha, and age, as well as influenced by mast cells. Collectively, these results demonstrate key links between immune response, arteriole remodeling, and vascular mediators and represent a novel mechanism of vascular modulation of immunity.

TABLE OF CONTENTS

LIST OF FIGURES

ACKNOWLEDGEMENT

There are many people I would like to thank for their support. First, I would like to thank my supervisor Dr. Geoffrey Payne for his guidance, support, and providing exceptional opportunities. I would like to thank my committee members, Dr. Sarah Gray, Dr. William Sessa, and Dr. Akiko Iwasaki for helpful discussions and direction. Special thanks also goes to Dr. Akiko Iwasaki for providing Tk$^-$HSV-2 virus and Melissa Linehan and other members of Dr. Iwasaki's lab for their work in aiding collaboration.

Members of the Northern Health Science Research Laboratory, both past and present, have been invaluable to me, with special note of the Gray Lab, K-Lynn Hogh, Elizabeth Dunn, and Dr. Andrea Gorrell. Additionally, the staff of the Northern Health Sciences Research Facility have been incredible and I sincerely thank them, including James Jones and Shannon Carrol, but, particularly Lydia Troc for her support and sharing her experience and expertise, and Dee Jones for always being accommodating and her dedication. Northern Medical Program support staff also deserves thanks; thanks to Judy Simms for keeping us safe, and Lindsay Mathews for making all things administrative run smoothly. Finally, I would like to express my gratitude to my friends and family for their unwavering support. In particular, thanks to my parents, Cindy and Steve Sellers, for always supporting my curiosity and pursuit of knowledge and to my brother, Scott Sellers, for finding the humor in every situation.

This work was supported by a UBC Medicine Seed Grant to Dr. Payne and UNBC Research Project Awards to Stephanie Sellers. Ms. Sellers was also funded by a CIHR Master's Award, an UBC Centre for Blood Research Studentship (Strategic Training Program – CIHR / HSFC), and a CIHR President's Fund Award.

CHAPTER ONE – GENERAL INTRODUCTION

1.1 Microvascular and Arteriolar Physiology

General Physiology

The microvasculature running throughout the body is a complex, vital network composed of arterioles, capillaries and venules. Traditionally, people associate microcirculation with the exchange of oxygen, nutrients, waste products, and hormones in vascular beds throughout the body, and generally, vessels less than one hundred micrometers in diameter are considered to be part of the microcirculation. A branch of a larger artery, arterioles consist of endothelial cells lining the lumen of the vessel (endothelium) and smooth muscle layer(s) wrapping around the vessel. The chief function of an arteriole is to maintain resistance within the microvascular network. Regulation of blood flow through arterioles occurs via vasoconstriction and vasodilation, which result from signals acting on the endothelium and smooth muscle cells (SMCs) as well as nervous system innervation. In a majority of tissues, arterioles are enervated by the sympathetic nervous system that influences vascular tone through nerve fibers. Postganglionic never fibers release norepinephrine, which predominately binds to alpha adrenergic receptors on SMCs and activates the phosphatidylinositol bisphosphate second messenger system leading to SMC constriction. The degree of constriction, or maintenance of homeostatic vascular tone, is determined by the level of norepinephrine. Alternatively, epinephrine, secreted from the adrenal medulla, has the ability to bind both alpha and beta-2 adrenergic SMC receptors, where beta-receptor activation leads to vasodilation through the production of cyclic adenosine monophosphate (AMP) (Germann & Stanfield, 2005). In general, this means that the degree of SMC activation,

and therefore the relative degree of vasoconstriction or dilation, is the vascular state required to maintain normal function and is a vessel's "set-point" under normal physiological conditions.

Vascular tone is a large factor in arteriolar networks, which arise from an initial branch from an artery. This primary branch is termed A_1 and ranges from 80 to140μm. Subsequent arterioles branching from the A_1 arteriole are termed A_2 (40 - 80μm) and A_3 (20 - 80μm) with arteriolar networks terminating into capillaries beds (Crijns *et al.*, 1998). Capillaries primarily function in allowing exchange between blood and tissues throughout the body. This task is facilitated by the highly branched nature of capillary networks that provides a large surface area that abets diffusion. Diffusion is also aided by the make-up of the capillary as the single layer of endothelial cells comprising capillaries makes rapid exchange with the target tissue possible. Following tissue perfusion, capillary beds collect into venular networks, which allow return of blood from capillary beds to venous circulation and return of blood supply to the heart (Greenberger, 1998).

Through the complete cycle, from heart to capillary bed and back, normal vascular function is required to maintain physiological homeostasis. Accordingly, vasculature will react dynamically, either through short or long-term responses to preserve functions within normal limits. To meet tissue demands in the short term, tissue perfusion is regulated by changes in vessel diameter by altering levels of smooth muscle cell (SMC) activation. Dilation is achieved via signaling within the SMC and ECs to induce a state of SMC relaxation and subsequent hyperemia. In addition to enervation, there are three main mechanism which facilitate SMC relaxation: nitric oxide (NO), endothelium-derived hyperpolarizing factor (EDHF), and protaglandin I_2 (PGI_2 or prostacyclin). When

produced in ECs of the arteriole, NO, EDHF, and PGI_2 lead to production of cyclic guanosine monophosphate (cGMP), opening of potassium channels with subsequent hyperpolarization of the SMC, and increased cyclic AMP respectively. Regardless of the upstream mechanism, all three induce a decrease in calcium ions in the SMC leading to vasodilation. Release of NO, PGI_2, and EDHF from the EC is triggered by an influx of calcium into the EC, with increasing intercellular calcium being a function of stimulation of receptors on the surface of the EC (Vanhoutte, 2003). Though many factors can activate ECs, a notable factor in EC activation within a study concerning changes in blood flow is shear stress. Blood flow within an arteriole generates shear stress on the vessel wall and changes in blood flow velocity will alter shear stress levels as it is proportional to the force applied to the vessel wall by the fluid moving through it and inversely proportional to the diameter. Therefore, increased shear stress causing EC activation and vasodilation acts to return shear stress to homeostatic levels. (Koller & Kaley, 1990, Koller Kaley, 1989). Vascular response to shear stress is achieved through mechano-sensors that include integrins such as $\alpha_v\beta_3$ and β_1, ion channels including those of calcium and potassium, G-proteins such as Ras, and receptor tyrosine kinases like Flk-1. Sensed changes in shear stress can result in a number of different physiological outcomes including EC proliferation, apopotosis, migration, and permeability (Li *et al.*, 2005).

Microvascular Adaptation

Changes in SMC activation state leading to vasodilation and vasoconstriction are primarily a short-term response, but to meet physiological demands in the long-term, vascular changes often take the form of structural adaptation or remodelling, in which

any or all of diameter, wall thickness, wall cross-sectional area, and wall to lumen ratio can be affected (Mulvany, 1999). Oxygen levels, cytokines, and metabolic demands can direct structural adaptation, but the largest factor directing adaptation is hemodynamics; blood flow is responsible for inducing shear stress on the vessel wall, while changes in transmural pressure result in alteration of circumferential wall tension (Pries & Secomb, 2002). Structural changes are categorized as hypotrophic, eutrophic, or hypertrophic. From their original state, vessels that exhibit no change in wall cross-sectional area are termed eutrophic, while those that show increased or decreased wall cross-sectional area are termed hypertrophic or hypotrophic respectively. An increase or decrease in cross-sectional area indicates a change in the amount of material within the wall (Mulvany, 1999), and changes in wall material can be the result of a number of mechanisms including EC proliferation, EC recruitment, mural cell recruitment, EC hypertrophy, or EC apoptosis (Dajnowiec & Langille, 2007, Li *et al.*, 2005, Yu *et al.*, 2005). These three forms of remodeling, eu-, hyper-, and hypo-trophic, can be further categorized as inward or outward remodelling. Inward remodelling refers to a decrease in lumen diameter, while an increase is termed outward remodelling (Mulvany, 1999).

In addition to structural adaptation, vascular changes can also take the form of increasing or decreasing blood vessel numbers or recruitment. Angiogenesis is the formation of new blood vessels. During angiogenesis, a number of factors act on ECs including fibroblast growth factor, angiopoietin-1and vascular endothelial growth factor (VEGF) (Ferrara *et al,* 2003, Ferrara *et al,* 1992, Leung *et al.*, 1989). Of these factors, VEGF is one of the most potent and critical growth factors implicated in arteriogenesis, increased diameter of existing arterioles or recruitment and expansion of collaterals,

vasculogenesis, de novo formation of blood vessels, EC division in stimulated LNs, and lymphangiogensis, formation of an increased lymph network (Ferrara *et al.*, 2003, Heil *et al.*, 2006, Nagy *et al.*, 2002, Webster *et al.*, 2006). Within the vasculature, VEGF is responsible for regulating EC proliferation, sprouting, migration, and survival as well as influencing vascular permeability mediated via interface with EC through binding to VEGF receptors 1 and 2 (VEGFR1, VEGFR2) on the EC surface. Ligand binding to the VEGF receptor induces oligomerization and activation through phosphorylation of residues within the oligomer. This then induces recruitment of intercellular signaling molecules to interface with the receptor complex and numerous down stream effects including factors that will be important considerations in this project such as changes in nitric oxide synthase activity, EC permeability, and EC proliferation (Stuttfeld & Ballmer-Hofer, 2009). The signaling cascade downstream of VEGF receptor activation is extensive. Generally however, interface with PLC-gamma leads to regulation of endothelial nitric oxide synthase and EC permeability. Meanwhile, activation of RAS, cSrc, and PI3K set off a signaling cascades that promote EC proliferation, EC migration and inhibition of apoptosis respectively (Ferrara *et al.*, 2003, Nieves *et al*, 2009).

Nitric Oxide

As evidenced above, vascular mediators are integral components of vascular function. One such mediator, which will prove to be integral to this project, is NO, an endothelium-dependent vasodilatory agonist. Constitutive NO within the vasculature is produced by endothelial nitric oxide synthase (eNOS), which produces NO through catalyzing the conversion of L-arginine to L-citrulline. However, other isoforms of NOS, namely neuronal NOS and inducible NOS, produce NO through the same conversion

(Sessa, 2004). Within the microvasculature, NO is noted to play key roles in regulating vasodilation, anti-coagulation, inflammation, vascular remodeling, and angiogenesis (Sessa, 2009).

NO induced vasodilation results from diffusion of NO from the endothelium to SMCs causing relaxation. This is primarily mediated through activation of guanylate cyclase, which in turn catalyzes the production of cyclic GMP from guanosine triphosphate (GTP). cGMP production activates potassium channels leading to SMC hyperpolarization and therefore, induction of a relaxed state (Vanhoutte, 2003). In addition to diffusion to act on SMCs, NO also diffuses into the lumen of blood vessels where it exhibits its anti-coagulation effects stemming from its ability to prevent platelet adherence and promote segregation of amassed platelets as evidence by decreased bleeding times and increased platelet adhesion in eNOS deficient mice (Freedman, 1999, Sessa, 2009, Vanhoutte, 2003). Beyond preventing the adhesion of platelets, NO also inhibits inflammatory cell adhesion, which will be detailed further in subsequent chapters in consideration of cellular trafficking cascades (Akimitsu *et al.*, 1995, Kubes, 1991, Martinelli *et al.*, 2009). Increased vascular leakage during inflammation is thought to be the result of NO, as genetic ablation of eNOS demonstrate decreased vascular leak. This inhibition is maintained with blockade of PI3K and Hsp90, positive regulators of NOS activity, or increased levels of caveolin, a negative regulator of NOS activity (Bucci *et al.*, 2005, Hatakeyama *et al.*, 2006). NO is also a key factor in the regulation of vascular changes induced by VEGF as mice deficient in eNOS lack the ability to respond to VEGF. Additionally, in ischemic conditions, loss of eNOS results in reduction in angiogenesis, arteriogenesis, and mural cell recruitment (Yu *et al.*, 2005). This may be

the result of the requirement of NO to stimulate endothelial cell proliferation in response to shear stress generated by high flow (Metaxa *et al.*, 2008). Alternatively, eNOS may be regulating VEGF levels as exogenous delivery of eNOS has been shown to increase VEGF expression and give rise to mature phenotype in newly formed arterioles and capillaries (Benest *et al.*, 2008). Collectively, these studies demonstrate the diverse role of NO in the vasculature and in facilitating changes in vascular physiology to meet physiological demand. Furthermore, the varied impact of NO on immune regulation will subsequently be presented, and when the roles of NO in the immune response and in vasculature are combined, supports investigation of NO in the LN and are detailed in Chapter 5.

1.2 Lymph Node Physiology

Lymph Node Function and Architecture

LNs are distributed throughout the body, ranging from cervical, to mesenteric, to inguinal, and popliteal. Generally, LNs are secondary lymphoid organs with the chief function of collecting antigen (Ag) and antigen presenting cells (APCs) from the periphery that present antigen to naïve lymphocytes that traffick to the LNs, thereby making LNs an intense site of immune activity (Murphy *et al.*, 2008). LNs serve as an interface between the innate and adaptive immune system. Pathogen associated molecular patterns (PAMPS) of infiltrating pathogens are sensed by a host and taken up by APCs in the periphery at the site of infection. While a variety to cells can be APCs, such as macrophages, ECs, and B-cells, they are most commonly dendritic cells (DCs), which are termed professional APCs. A variety of DCs exist; DC subsets are defined by their surface antigens, and differ based on tissue localization and mechanisms of capturing and

processing antigen. The main class of DCs that is associated with LNs is the conventional DCs (cDCs) class. Migratory cDCs exist in an immature state in the periphery and subsequently mature and migrate through the lymph into the draining LN and present antigen on major histocompatibility complex (MHC) molecules following internalization of antigen. Alternatively, free antigen can be transported to the lymph node and processed and presented in the LN by resident or blood-derived cDCs (Randolph *et al.*, 2005, Villadangos & Schnorrer, 2007, Murphy *et al.*, 2008).

Once antigen is presented, the search for rare cognate T cells begins. Given the vast diversity of T-cell receptors, only one in 10^5 to 10^6 cells in a mouse are specific for a given antigen, the rapidity of this process is vital to quick on-set of adaptive immune response (Casrouge *et al.*, 2000). Screening of naive T cells within the LN is dependent upon T cells numbers, blood supply to the LN, density of DCs within the node, and antigen dose. If a naïve T cells is cognate, it will remain in the lymph node and undergo clonal expansion, but most cells entering the LN are not cognate and return to the circulation though efferent lymph vessels. Successful DC interaction with a cognate naïve T cell occurs in three phases and is dependent on cytokine expression and co-stimulatory molecules (Henrickson, 2008, Soderberg, 2005). Following clonal expansion, lymphocytes acquire effector cell functions, which are antigen specific, thereby inducing an adaptive response specific to the invading pathogen, and are critical for fighting infection. The process of amassing naïve T cells within the LN during the on-set of adaptive immunity results in LN hypertrophy, however, this state of increased cellularity and swelling resolves (Murphy *et al.*, 2008, Soderberg *et al.*, 2005).

Whether in a state of hypertrophy or not, the internal structure of the LN is distinctly organized with two main divisions: the cortex and the medulla. The cortex is segmented into a paracortex or T cell area surrounded by a B-cell area in the outer cortex. The T cell area is the main site of screening for cognate T cells and subsequent activation and proliferation. The B-cell area is comprised of primary follicles and germinal centers where activated B cells proliferate and differentiate. The medulla is made up of sinuses that drain the lymph and are separated by medullary cords. While a variety of cells have been noted to reside in medullary cords, such as plasma cells and macrophages, the role of the medulla is yet to be clearly understood (von Andrian, 2003).

Lymph Vascularization

The microvasculature interacts with and influences the immune system in a variety of ways from expression of regulatory cytokines, to cell trafficking, impact of flow dynamics, and supply of metabolites. Therefore, continuing to elucidate the interface between the immune and microvasculature systems is important and LNs are an excellent choice for exploring such immune-microvascular interaction, as they are highly vascularized and key for rapid induction of host-defense mechanisms. In addition to having a highly complicated internal structure, lymph nodes also have a well-defined and complex vasculature. The vasculature of the LN can be divided into a number of pieces with the main feed arteriole being the upstream supplier of blood. This arteriole branches into a capillary network and then into specialized post-capillary venules that feed the LN. These post-capillary venules are known as high endothelial venules (HEVs). HEVs consist of a single layer of cuboidal endothelial cells specialized to facilitate movement of cells into the LN. HEVs occur at in the centre of paracortical cords and occur most

frequently in T-cell zones to optimize delivery of blood borne lymphocytes during homeostatic immune surveillance and induction of adaptive response. HEVs are surrounded by layers of fibroblastic reticular cells (FRCs), and unlike normal venules, they have a thick basal lamina and notable perivascular sheath (von Andrian & Mempel, 2003, Murphy *et al.*, 2008, Miyasaka & Tanaka, 2004). The endothelium of HEVs is critical to successful lymphocyte migration into the LN (Marchesi & Gowans, 1964) and extensive research regarding signaling molecules and chemokine expression patterns in HEVs, which enable cell trafficking both in the presence and absence of infection, have been conducted and are discussed below.

Lymph Node Trafficking

The general trafficking cascade in all tissues involves rolling, activation, adhesion, and transmigration. Within peripheral LNs, rolling is mediated by the expression of highly glycosylated and sulphated sialomucins known as peripheral node addressins (PNAds) on the HEV. Lymphocytes targeted to LNs express L-selectin, which bind to PNAd (Ley *et al.*, 2007, Miyasaka & Tanaka, 2004). Notably, the expression of PNAd is itself regulated as PNAd levels have recently been shown to be controlled by expression of lymphotoxin-β receptor (LTβR), with blockade of LTβR leading to decreased cellularity in reactive lymph nodes (Browning *et al.*, 2005). Following rolling, activation involves the interaction of CC-chemokine receptor 7 (CCR7) with CC-chemokine ligand 21 (CCL21) and CCL19 as well as the interaction of CXC12 with CXCR4. This type of interaction, chemokine binding to a chemokine receptor initiates intercellular signaling via the Giα pathway, which leads to conformation changes that allow adhesion or arrest to be achieved. In the LN, this occurs by leukocyte function-associated antigen (LFA-1)

binding to intercellular adhesion molecules (ICAMs). Importantly, it is this trafficking cascade that allows selective recruitment to the LN. For example, L-selectin is not expressed in effector memory T cells therefore they fail to roll along the endothelium and do not migrate into the LN and while myeloid cells can roll as they typically express L-selectin, they fail to arrest to the absence of CCR7 or CXCR4 (Ley *et al.*, 2007, Miyasaka & Tanaka, 2004, von Andrian & Mempel, 2003). L-selectin expression is particularly important in terms of $CD4^+$ T cell trafficking to draining lymph nodes during induction of adaptive response; L-selectin is required for naïve T cell migration into LN as systemic treatment with antibody against L-selectin prevents accumulation of naïve $CD4^+$ T cells (Bradley *et al.*, 1994).

Blood flow is also a factor to consider within the lymphocyte trafficking cascade as leukocytes within the blood flow at a rate of 1-10mm/s, which is too fast for migration and therefore dictates the need for selectin mediated adhesiveness along the vessel wall. Interaction with the vessel wall is also impacted by blood flow, as it is known to influence the arrangement of leukocytes within vessels as well as regulate cellular rolling speed along the endothelium; in states of high flow and shear rate, leukocytes are buffered away from the vascular endothelium and have a rolling speed too high for optimal trafficking (Kubes *et al.*, 1991, Ridger *et al.*, 2008). Conversely, the absence of flow has been shown to cause rolling lymphocytes to disengage from the endothelium, a phenomenon known as the 'shear threshold effect'. This phenomenon refers to the maximal binding of L-selectin to PNAd at $1dyn/cm^2$, and drops significantly below $0.6dyn/cm^2$. This effect is largely specific to L-selectin, but is worth serious consideration as L-selectin is a key mediator of naïve T cell trafficking into peripheral lymph nodes.

(Finger *et al.*, 1996). Shear stress is also associated with changes in expression levels of adhesion molecules on the vascular endothelium as well as the stability of interaction between such adhesion molecules and integrins on the surfaces of migrating T cells. A LN specific example of this is lymphocyte function-associated antigen-1 (LFA-1) and intercellular adhesion molecule-1 (ICAM-1); the activation of LFA-1 to a low affinity extended state from a bent low affinity conformation is promoted through the chemokine CCL21. Notably, CCL21 immobilized on the endothelium is hypothesized to silence integrins in the absence of force generated by flow. Subsequent to the conversion to a low affinity extended state, the force of flow within a vessel is then also responsible for converting a LFA-1 to a high-affinity extended conformation, thereby allowing engagement of ICAM-1 and arrest on the endothelium. (Sucosky *et al.*, 2009, McEver & Zhu, 2007, Alon & Dustin, 2007).

As previously discussed in relation to vascular function, NO is a mediating factor in blood flow regulation and therefore has an indirect impact on trafficking within the LN via altered hemodynamics. However, NO also has direct impact on trafficking. NO has been shown to attenuate leukocyte adhesion to endothelium. This presented targeted treatment with exogenous NOS inhibitors such as a possible mechanism to influence leukocyte adhesion, and was subsequently demonstrated by Kubes and colleges (1991) whom showed a 15-fold increase in leukocyte adherence in post-capillary venules following treatment with NOS inhibitors L-Nitro-Arginine Methyl Ester (L-NAME) and N-Methyl-L-arginine acetate (L-NMMA). Increased adherence was also accompanied by higher rates of emigration and decreased venular shear (Kubes, 1991, Akimitsu *et al.*, 1995). Inhibition of NOS has also been shown to further increase leukocyte rolling in

sepsis, wherein rates of rolling and adhesion are already high, and was reversible by administration of L-arginine (Sundrani *et al.*, 2000). This suggests that exogenous supply of L-arginine may be useful in increasing the bioavailability of NO in states of adverse immune reaction and could potentially be used to aid NO production and inhibit lymphocyte adhesion. Additionally, recent studies provide evidence that NO may also promote lymphocyte transmigration through stimulation from ICAM-1 (Martinelli *et al.*, 2009) with the ability of some leukocyte subsets to bind ICAM-1 and mediate adhesion demonstrated to be NO dependent (Norman *et al.*, 2008).

1.3 Changes in Lymph Node Vasculature & Study Objectives

Vascularization During Immunization

The question of how antigen stimulation causes an increase in trafficking of lymphocytes from the blood has been asked for decades. Studies aimed at answering this question have generally fallen into two categories: those looking at increased recruitment into the lymph node, and those looking at increased blood flow to the lymph node. The first, increased cellular recruitment, refers to the ability of the immune system to interact with lymph node microvasculature to create a microenvironment that favors movement of circulating lymphocytes into the lymph node thereby increasing the percentage of cells transmigrating into the node. As detailed above in the discussion of lymph node physiology and lymphocyte trafficking, this is a complex interplay of adhesion molecules, selectins, chemokines, and receptors. The second, increased blood flow, is as of yet, less defined. Early studies using radiolabeled microspheres showed increased blood flow to draining lymph nodes which mirrored lymph node weight during immune response (Hay & Hobbs, 1977). Additional studies using microangiography of rabbit LNs

showed vascular changes beginning in the subcapsular and medullary cords within the first day of antigen challenge that peaked at day five. This vascular growth was subsequently shown to involve the LN cortex by day three, facilitating vascularization of the hypertrophied LN and germinal centers. Despite this vascular expansion, microvasculature returned to normal by day seven (Herman *et al.*, 1972) and the author's theorized that areas within the LN with increased blood flow was the result of shunting and vessel rearrangement, not angiogenesis. However, further study of vascularization of LN using LNs draining skin allografts demonstrated increased length of HEVs and HEV arborization (Anderson *et al.*, 1975).

More recent studies of LN vasculature have begun to further elucidate changes in LN vasculature at the HEV level. HEVs are noted to exhibit plasticity in terms of expression of addressins and morphology in response to changes in flow dynamics and gene expression (Browning *et al.*, 2005, Hendriks *et al.*, 1987), with Hendriks and colleges reporting decreased endothelial surface area and flattening of ECs in response to limiting afferent lymphatic flow (Hendriks *et al.*, 1987). But, when considering HEV alteration in the context of immunization, early reports note dilation of HEVs as indicated by increase in cross-sectional area and accompanied by increased EC size within the vessel (Myking, 1980). However, a number of studies support HEV proliferation over dilation; Mebius and colleges (Mebius *et al.*, 1990) show increased HEV staining within the LN T cell zone during immunization, and Soderberg and colleges report that HEV do not increase in size, but instead increase in number proportional to lymph node size and cellularity during challenge with herpes simplex virus type II (Soderberg *et al.*, 2005).

A number of mechanisms are proposed for regulating LN vasculature at the level of the HEV. Liao and Ruddle (2006) demonstrate HEVs and lymphatic vessels exhibit synchronistic plasticity and remodel during immunization through B cell and LTβR cross-talk. Subsequent studies demonstrated B cells to be specific to expansion of the LN lymph network and migration of DCs to the LN (Angell *et al.*, 2006). Other studies later identified LTβR to be a regulator of fibroblast-type reticular stromal cell (FRC) production of VEGF in the lymph node (Chyou *et al.*, 2008), a study based on previous findings that VEGF levels within the LN were responsible for vascular growth. Notably, VEGF is known to be expressed or induced by a variety of immune cells including B cells, DCs, and T cells (Ruddell *et al.*, 2003, Webster *et al.*, 2006, Zhao *et al.*, 2004), but in direct study of vascular growth of HEVs, as was indicated by EC proliferation, VEGF expression was demonstrated to be dependent on DCs in the LN (Webster *et al.*, 2006). Most interestingly perhaps, in accordance to the relation to LN cellularity and rapid induction of adaptive immune response, blockade of LTβR or decrease in DC numbers was sufficient to decrease VEGF levels and EC proliferation within the LN, resulting in decreased cellular accumulation (Chyou *et al.*, 2008, Webster *et al.*, 2006).

Despite the number of studies on general increase in blood flow to LN and vascular expansion within the LN at the HEV and lymphatic drainage levels, there is a paucity of information in regards to how blood flow to the LN and HEVs during immunization is accomplished upstream. In fact, the only study to specifically address this question identified the LN feed arteriole to be the key upstream regulator. This study showed that three days post-infection with herpes simplex type II there is significant remodeling to a larger arteriole diameter, which was recorded to be fifty percent larger than prior to

infection. Such an increase allowed increased blood flow and supply of naïve T cells to the LN, and thereby increased the rate of screening for rare cognate lymphocytes from 3 x 10^6 cells/day, which has been noted in a naïve mouse, to 14 x 10^6 cells/day. Increased arteriole diameter was also noted to correspond with cellular accumulation and HEV proliferation (Soderberg *et al.*, 2005).

Study Objectives

Study of changes to the LN feed arteriole by Soderberg and colleges (2005) effectively demonstrated the existence of an integral link between the immune system and microcirculation in the LN at the arteriolar level. Given the correlation between increase in arteriole size, lymph node cellularity, and HEV number and blood flow, the regulation of blood flow upstream of HEV within the LN most probably has an impact on downstream vasculature, and therefore, could regulate cellular trafficking and the induction of adaptive immune response. While suggestion of such a link is novel within the LN, the concept of the control of upstream events on downstream outcomes is not; history has shown us that understanding what is located above the direct point of interest, such as in signaling cascades, or perhaps more relevantly as in hyperemia to peripheral inflammatory sites or active muscle, can provide new insight into downstream events and potential therapeutics avenues, and thereby speaks to the importance of further understanding upstream regulation of LN vascularization. Therefore, in an effort to understand and explore therapeutic applications of changes in arteriolar vascularization of the LN during immune response, this project aims to study the LN feed arteriole in order to address many important and as of yet unanswered questions that must be addressed. To this end, the main objectives of this study are:

(i) To elucidate the extent and nature of vascular remodeling within draining lymph nodes during infection upstream of HEVs at the arteriolar level and consider the potential impact of such remodeling on health and disease.

(ii) Begin to elucidate the mechanism of draining lymph node vascular remodeling in order to identify future targets for control of LN vascular supply.

In meeting these objectives, the hypothesis that arteriole remodeling is a phenomenon driven by vascular and immune mediators that is observed throughout the course of infection to increase blood flow to the LN and facilitate adaptive immune response on-set will be addressed. In turn, data that address such a hypothesis will provide new and vital insight into LN vascularity and its impact on cellular trafficking and induction of effective immune response. Furthermore, it will be a starting point from which to continue to dissect the mechanism of arteriole remodeling within the lymph node and begin to appreciate its immune regulatory action and resulting therapeutic potential and represents an interdisciplinary approach linking immunity, vascular physiology, and microcirculation in the context of infection.

CHAPTER TWO - METHODOLOGIES

2.1 Herpes Simplex Virus Type II Pathogenesis

Herpes Simplex Virus Type II (HSV-2) was used as an infection model throughout experiments. HSV-2 represents an excellent and significant model in which to study vascular changes during infection, as it is a physiologically relevant model of a sexually transmitted infection (STI). STI's are a significant area in that they continue to be a pathological burden throughout the world; In fact, globally, the infection rate of sexually transmitted infections is staggering and exceeds 400 million adults per year. HSV-2 itself is estimated to infect one in every five individuals in the USA alone and can manifest as genital herpes as well as frequently fatal neonatal disseminated herpes or herpes encephalitis (Fleming *et al.,* 1997, Handsfield *et al.,* 1999). Notably, the development of genital herpes is also an important cofactor in HIV-1 transmission via increased numbers of T cells and DCs susceptible to HIV-1 infection during and following HSV-2 ulcerations (Zhu *et al,* 2009). This association thereby makes HSV-2 infection rates a contributing factor to the global HIV pandemic (Cameron *et al,* 1989, Stamm *et al,* 1988, Freeman *et al.,* 2006), which presents an alarming threat to human lives and highlights the need for further study of STI's in general and supports the use of HSV-2 as an infectious model for this study. Furthermore, the persistence of STI's also speaks to a need to use multi-faceted studies to appreciate different interacting aspects of sexually transmitted infections in order to expand our understanding of pathogenesis and/or elucidate potential new therapeutic avenues (Medzhitov, 2009). Additionally, using an infection model such as HSV-2 is useful as it is well established and any observed

changes or phenotypes within the vasculature will be able to be correlated with what is already known about HSV-2 pathophysiology.

The general pathophysiology of HSV-2, a member of the herpesviridae family, demonstrates it to most commonly manifest as genital herpes and present clinically with vesicular lesions and pustules on the epidermis within two to ten days from primary infection. The virus infects and replicates in the mucosal epithelial cells as well as in neurons innervating the infected area. Neurons are also the site of HSV-2 latency, specifically the sacral root ganglia, thereby establishing a viral reservoir for the virus that enables recurrence. Although both humoral and cell-mediated immunity are mounted during infection, these responses are not sufficient to clear the virus. Currently, there is no vaccine against HSV-2, and treatment for individuals infected is the use of anti-viral agents, such as Acyclovir. However this treatment does not clear the virus, but does work to decrease symptom severity and frequency of recurrence (Greenberger, 1998).

Upon infection of the genital mucosa with HSV-2, the virus is recognized by components of the innate immune system. Given the high number of CpG motifs in the HSV-2 genome, HSV-2 is most frequently recognized through TLR 9 by antigen presenting cells (APCs) within the genital mucosa (Lund *et al.*, 2003, Sato *et al,* 2006). Antigen presenting cells then traffic to and present antigen in the draining lymph nodes (Murphy *et al.*, 2008). The draining lymph nodes of the genital mucosa are the iliac and inguinal lymph nodes and are the site of induction of adaptive immune response to an HSV-2 infection of the genital mucosa. Conveniently, HSV-2 can be given intra-vaginally (i.vag.) in murine models, which opens the possibility of studies to using a host of murine genetic models, and allows the study to be conducted within a biologically

relevant infection route as HSV-2 given i.vag. will drain the inguinal lymph node, which is an accessible and established site of intravital microscopy (IVM) study of LN vasculature (Soderberg *et al.*, 2005, Overall, 1975).

2.2 Infectious Model & Immunization Protocol

To achieve consistent infection, mice were treated with Depo-Provera (medroxyprogesterone acetate at 5mg/mouse) five to seven days prior to infection by subcutaneous injection in the ruff of the neck; Depo-Provera induces a diesterous phase and significantly increases susceptibility to HSV infection (Baker *et al.*, 1978, Kaushic *et al.*, 2003). Subsequently, Depo-Provera treated female mice were intravaginally (ivag) infected with 10^6 pfu of thymidine kinase mutant HSV-2 strain 186TKΔKpn (TK$^-$HSV-2). Virus was diluted in sterile phosphate buffered saline (PBS) to give a concentration of 10^6pfu/10μl. Prior to infection, mice were given a dose of sodium pentobarbitol (90mg/kg by i.p. injection). The vaginal mucosa was then swabbed with a calcium alginate swab moistened with sterile phosphate buffered saline (PBS). Virus was then introduced via pipette tip and the mouse was propped with its hind end upwards for approximately twenty minutes and allowed to recover from anesthetic.

TK$^-$HSV-2 was a generous gift from Dr. Akiko Iwasaki at Yale University School of Medicine with permission for use given by Dr. David Knipe at Harvard Medical School. Virus was propagated by inoculation of Vero cells with virus stock and then allowing for viral replication. Cells were then harvested and lysed by sonication. Viral titer on the lysate was determined in plaque forming units (pfu) using Vero cells. The same viral stock was used throughout the project and had a titer of $1x10^9$pfu/ml. Tk$^-$HSV-2 is an attenuated strain of HSV-2 that lacks the thymidine kinase gene, which prevents

reactivation of the virus from latency and is non-lethal to mice. From a vascular study perspective this is important as it allows for the vasculature to be studied for a lengthy period without worrying about mortality to the animal, as well as allows focus on a single infectious event opposed to determining if a vascular response was due to the primary infection or recurrence. Furthermore, TK⁻HSV-2 is sufficiently immunogenic that subsequent immunization with wild-type virus shows mice to be resistant to rechallange as demonstrated by a 10-fold increase in lethal dose of virus. This means that the same model could be used to study vascular changes during re-challenge in the future (McDermott *et al.,* 1984, Jones *et al,* 2000, Parr *et al.*, 1994).

2.3 Intravital Microscopy

While progress is being made in developing alternative techniques, intravital microscopy (IVM) has long served as a vital tool in visualizing immune response *in vivo.* IVM has been conducted in a multitude of tissues including pancreas, brain, skeletal muscle, liver, and lymph nodes. In terms of the type of IVM used to study the microvasculature, our group has found in practice that while two-photon offers advantages in the depth of tissue that can be imaged as well as the increased data analysis capabilities, bright-field and epi-fluorescent IVM have greater flexibility in the location of preparation due to a lack of need for water or oil immersion, complete immobilization of the preparation area, or a flat preparation allowing for cover slip application. Regardless of the type chosen, intravital microscopy is an indispensable tool in studying vasculature *in vivo.* It provides for real-time, *in vivo* imaging; the result of a disease process or new therapeutic on tissue function can be directly visualized. In terms of vascular supply, it allows for study of vessel functionality, flow dynamics, integrity, and

vessel number among others, all in the *in vivo* context which the vasculature functions everyday. Most importantly for this study, IVM lends itself well to use at further investigating microcirculation in immune response in terms of LN vascularity due to the existence of preparations of a number of lymph nodes including the popliteal, cervical, and inguinal nodes (Sumen *et al,* 2004, Mempel *et al,* 2004, Germain *et al.*, 2006). In this study a preparation of the inguinal lymph node was utilized, as it is a draining lymph node for infection of the vaginal mucosa. Animal preparation, surgical procedure, and methods for creating a profile of the vasculature are given below.

Animal preparation. Sodium pentobarbitol was administered at an initial dose of 90mg/kg by intraperitoneal (i.p.) injection. Drug effect was monitored throughout the experiment by via response to toe pinch. Subsequent doses of drug were given as needed at 20mg/kg. Hair was shaved from the abdomen and hip area of the mice and swabbed with alcohol . Mice were subsequently placed supine on a clear custom surgical board.

Surgical Procedure. Surgical procedures were performed under a standard dissecting microscope. A midline incision was made along the ventral surface of the abdominal cavity and the skin was retracted towards the spine. The resulting skin flap was pinned onto a clear Sylgard 184 pad. Subsequently, the layer of connective tissue surrounding the LN was removed and overlaying adipose tissue was cleared until the microvasculature was exposed. When required, the main lymph node venule was manipulated to allow visualization of the main feed arteriole (Figure 1). Throughout the surgical preparation, tissue was constantly kept moist with bicarbonate-buffered physiological salt solution (PSS) (pH 7.4, 37°C, 131.9mM NaCl, 4.7mM KCl, 1.2mM

$MgSO_4$-$7H_2O$, 2mM $CaCl_2$-$2H_2O$, 18mM $NaHCO_3$) that had been equilibrated with 5% CO_2 - 95% N_2 for at least one hour.

Figure 1: Inguinal Lymph Node Preparation. Schematic diagram of intravital microscopy preparation of the inguinal lymph node feed arteriole with progression shown from left to right. First, the mouse is place supine and a midline incision is made and dissected back towards the spine to create a skin flap. The flap is made and pinned out to expose the lymph node and the overlaying fat pad. Finally, the overlaying fat pad and connective tissue is dissected to reveal the lymph node arteriole (red) and venule (blue).

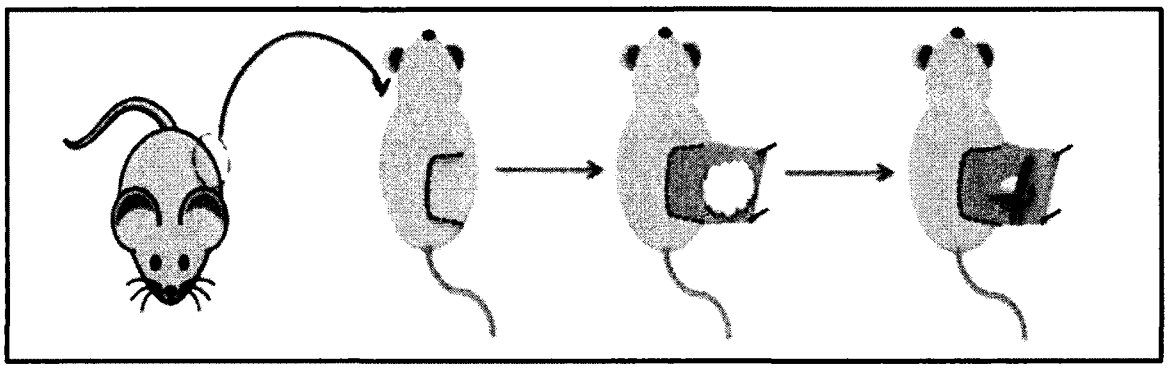

Vasoactive profiles. Once completed, the preparation was secured on a modified Nikon Eclipse intravital microscope and the feed arteriole was observed at a total magnification of 950× using video microscopy. The preparation was constantly superfused with PSS maintained through a water-jacket heated reservoir at 32-37°C. Vessel diameters were determined from the width of the red blood cell column using a video caliper. The same vessel segment was studied in each mouse per group. The resting vessel diameter was measured following sixty minutes of equilibration with PSS. The effect of a smooth muscle-specific agonist phenylephrine (PE) (Sigma-Aldrich, catalog #P6126) was evaluated by cumulative addition (1nM to 10μM) to the superfusate. At each concentration, the stable arteriolar diameter was recorded before the next increment. The preparation was then superfused with control PSS to recover for approximately thirty-five minutes and additional agonists were subsequently evaluated. When the preparation was equilibrated with L-NAME to inhibit NOS, L-NAME was prepared fresh at 100μM (pH 7.4) in PSS and superfused over the preparation for sixty minutes with vessel diameter recorded at 0, 30, 45, and 60minutes. Maximal vessel diameter measurements were obtained by equilibrating the preparation with 100μM sodium nitroprusside (SNP, Fluka, catalog #71780) or 30μM Nifedapine (Sigma-Aldrich, catalog #N7634). A representative image of the IVM imaging set-up and typical image projected from the IVM microscope is given below (Figure 2A,B) (Sellers & Payne, 2011). In cases where fluorescence was used for imaging of the lymph node feed arteriole, 1% w/v fluorescein isothiocyanate dextran (FITC-dextran) was prepared in 1X sterile phosphate buffered saline (Invitrogen, catalog #20012043). FITC was given inter-cardiac at a dose of 100μl per mouse and allowed to circulation for approximately ten minutes prior to imaging. Imaging was

conducting using filters and a mercury lamp adapted to the IVM scope used in all other experiments. At the end of IVM imaging, mice were euthanized by overdose of sodium pentobarbitol followed by cervical dislocation.

Figure 2: Intravital Microscopy Lymph Node Imaging. A. Typical IVM microscope set-up. **B**. IVM image of inguinal lymph node feed arteriole (red arrow and red false colouring) feeding the lymph node equilibrated with physiological saline solution and running along side the main venule (green arrow). Images are frames from Sellers & Payne, 2011.

A

B

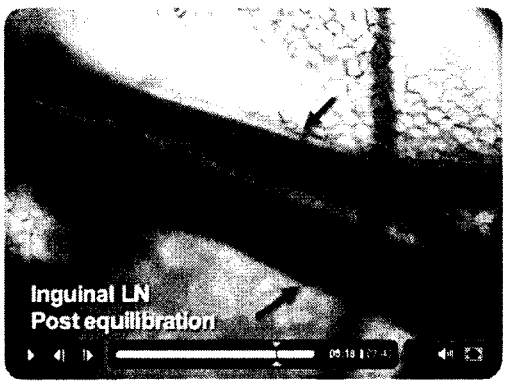

2.4 Animal Models and Animal Care & Use

Mice models were used throughout as the IVM model of the inguinal lymph node used in initial previous studies (Soderberg, 2005) relied on murine models, and murine models provide a number of important genetically manipulated models to use in dissecting the mechanism of vascular changes in the LN. C57 BL/6J mice (WT, stock #000664) were used as a wild-type base and were purchased from The Jackson Laboratory (Bar Harbor, Maine). For genetically manipulated mouse models, $CD4^+$ T cell deficient mice ($CD4^{-/-}$, B6.129S2-CD4<tm1Mak>/J, stock #002663), endothelial nitric oxide synthase deficient mice ($eNOS^{-/-}$, homozygous B6.129P2-NOS3<tm1Unc>/J, stock #002684), mast cell deficient mice (compound heterozygous WBB6F1/J-Kit<W>/Kit<W-v>/J, stock #100410), caveolin-1 deficient mice (homozygous cav1<tm1Mls>/J, stock #004584), and tumor necrosis factor alpha deficient mice ($Tnf\alpha^{-/-}$, homozygous B6.129S-Tnf<tm1GK1>/J, stock #005540 were purchased from The Jackson Laboratory. Additionally, homozygous $eNOS^{-/-}$ breeder pairs were also purchased from The Jackson Laboratory and bred in the Northern Health Sciences Research Facility (NHSRF) at UNBC. Mice deficient in L-selectin (L-$selectin^{-/-}$) were a generous gift from Dr. Klaus at the La Jolla Institute for Allergy & Immunology. Adult mice were used at 8 to 20 weeks of age. Mice were considered old at greater than 18months of age. Regardless of strain, all mice used were female given that virus was administered intra-vaginally.

All mice were housed for a minimum of one week after arrival at the NHSRF at UNBC before experimental use to eliminate effects due to stress of shipping. Mice were housed at 22°C in with a 12 hour light / 12 hour dark cycle and were permitted free access to food (Rodent *LabDiet* 5001) and water. They were inspected daily for adverse

reactions to experimental treatments and used at $\geq$ 8 weeks of age. All procedures were approved by the University of Northern BC Animal Care and Use Committee (approved under current protocol A2010.0924.03(1)).

2.5 Pharamcological treatments

In order to support results from genetic ablation models, pharmacological treatments were used. Specifically, in the cases in which $CD4^+$ T cells and eNOS were ablated, pharmacological systemic treatment with antibody against CD4 and systemic treatment with a global nitric oxide inhibitor were used respectively.

CD4 Depletion. Female C57 BL/6 mice were used for $CD4^+$ T cell depletion studies. Mice were treated with antibody by intraperitoneal injection of 0.2mg of functional grade anti-mouse CD4 (L3T4, eBioscience, catalog #16-0041). Initial injections were given four days prior to infection and were repeated two days prior to and two day after infection. This protocol has previously been demonstrated to be effective for $CD4^+$ T cell depletion in the context of HSV-2 infection by Dr. Yusuke Nakanishi in Dr. Iwasaki's laboratory. However, similar protocols have also be shown to be effective in depleting circulating $CD4^+$ T cells in the context of infectious models by other groups (Wozniak *et al.*, 2011, Matloubian *et al.*, 1994) including during HSV infection of C57 BL/6 mice (Jennings *et al.*, 1991).

L-NAME Treatment. Female C57 BL/6 mice were treated with Nitro-L-arginine methyl ester hydrochloride (L-NAME, Sigma-Aldrich, catalog #N5751). L-NAME was dissolved in drinking water at a concentration of 0.5mg/ml changed daily. This method has been shown to be effective at blocking NOS expression in the context of vascular remodeling and lymphocyte accumulation in asthma models in the lung the by Bhandari

et al. (2006). Treatment was administered for fourteen days prior to initial treatment with Depo-Provera and continued throughout the course of Depo-Provera treatment and infection.

2.6 Histology & Tissue Samples

Tissue samples were collected for further analysis. Tissues collected included inguinal and iliac LNs and individual lymph node feed arterioles. LNs were collected from euthanized mice and stored in 5% buffered formalin. Lymph node feed arterioles were collected from anesthetized mice; once exposed, the lymph node feed arteriole was briefly superfused with 100μM SNP to induce maximal dilation and then was superfused with 5% buffered formalin and clamped with forceps. The arteriole was then carefully dissected out and stored in 5% buffered formalin. Arterioles used for IVM imaging and treated with vaso-active drugs such as phenylephrine or L-NAME were not used for tissue collections.

Feed arteriole samples were shipped to Wax-it Histology Services Inc. (Vancouver, BC, www.waxitinc.com) for paraffin embedding, sectioning and staining. For each data point, a minimum of three arterioles from separate animals were processed. Sections were imaged using a standard light microscope.

2.7 Statistical Analyses

All statistical analyses were performed with GraphPad Prism 5.0 (GraphPad Software, San Diego California USA, www.graphpad.com). Data was analyzed using one-way and two-way repeated-measures analysis of variance with Bonferroni and Dunnett's Multiple Comparison post tests, and paired T-tests with statistical significance

defined as *$p<0.05$, **$p<0.01$, and ***$p<0.001$. Specific N-values for arteriole diameters and response to vaso-active drugs are all greater than or equal to three, with specific N-values given in each figure.

CHAPTER THREE – Vascular Profile of Lymph Node Feed Arteriole During Infection

3.1 Introduction

Elucidating the mechanisms controlling the on-set of adaptive immunity is an ongoing goal of researchers across the globe as every new aspect of understanding presents novel therapeutic insights into how to initiate an adaptive response more quickly and/or robustly. Previous research on induction of adaptive immune response has often focused on LNs, as they are the main sites of antigen presentation by APC to naïve T cells (Murphy *et al.*, 2008). In fact, given the rarity of antigen specific naïve T cells, approximately only 20-200 $CD4^+$ T and 20-1200 $CD8^+$ T cells in a C57 BL/6 mouse are antigen specific, the search for cognate lymphocytes by APC in LNs is rate-limiting in production of effector cells needed to fight infection (Obarr *et al.*, 2010, Obarr *et al.*, 2008), with the time required for the production of T_h1 effector responses being inversely proportional to the number of cognate lymphocytes in the LN (Soderberg *et al.*, 2005). Therefore, based on the scarce nature of cognate lymphocytes, most past studies aimed at understanding induction of robust adaptive response have focused on determining factors that allow for efficient screening of lymphocytes within the LN. Subsequently, given that a high screening rate for cognate T cells would necessitate high input, and that the majority of trafficking cells enter the LN from the blood and exit through the afferent lymph (Hall, 1974, Hay & Hobbs, 1977), studies of LN vascularity are common within those examining adaptive immune response on-set.

Vascularity studies within reactive LNs began with general reports of hyperemia and identification of areas within the LN with increased vascularization (Hay & Hobbs, 1977, Herman *et al.*, 1972). Studies then progressed to focus on specific vessel types,

with the majority of studies centering on HEVs. This led to an extensive understanding of homing and trafficking across HEVS (von Andrian & Mempel, 2003) and conflicting reports of HEV expansion, proliferation, and arborization (Anderson *et al.*, 1975, Liao & Ruddle, 2006, Mebius *et al.*, 1990, Myking, 1980, Soderberg *et al.*, 2005). However, the impact of upstream microvasculature, at the level of the feed arteriole, in the immune response remained unexplored prior to a recent study by Soderberg and colleges (2005), which demonstrated that lymphocyte accumulation occurred as a result of an increase in blood supply via expansion of the primary feed arteriole to the draining LN; The LN arteriole remodeled to an ~50% greater diameter three days post-immunization (p.i.) with Herpes Simplex Virus Type II (HSV-2). Such an increase in blood flow into the LN would theoretically increase the rate of screening for rare cognate lymphocytes from $3x10^6$ to $14x10^6$ cells/day (Soderberg *et al.*, 2005), which given the rate-limiting nature of screening for cognate lymphocytes, justifies further study of arteriole remodeling.

Arguably, the best place to begin is to investigate LN arteriole remodeling further is to determine the kinetics, magnitude, and nature of remodeling as understanding these characteristics would better allow for links to be make to what is already known about immune and vascular response within reactive LNs. For example, in the case of HSV-2 infection in the genital mucosa, presentation of antigen occurs on MHC II to naïve $CD4^+$ T cells in the inguinal and iliac lymph nodes by DCs migrating from the periphery into the LN through lymphatics within hours of immunization (Greenberg *et al.*, 2008, Kumamoto *et al.*, 2011Soderberg *et al.*, 2005). This is followed by screening of cognate lymphocytes and cellular accumulation within the lymph node with increased cellularity and LN hypertrophy noted to continually increase until at least five days following

infection (Soderberg *et al.*, 2005). Successful induction of adaptive immune response gives rise to primed $CD4^+$ and $CD8^+$ effector cells which begin migrating into the infection site at days three to four and four to five respectively following infection (Nakanishi *et al.*, 2009), with subsequent resolution of LN hypertrophy. If the profile of LN arteriole expansion does not correspond to the dynamics of the immune response noted above, this would suggest a mechanism driving expansion independently of those involved in induction of adaptive response in the LN. However, the opposite is also a possibility; correlation to the timeline of immune response to HSV infection would suggest an immune based mechanism driving arteriole expansion.

An immune driven mechanism following the course of infection is also supported by studies of HEVs as changes in HEVs following the course of infection are dependent upon B cells and DCs (Angell *et al.*, 2006, Liao & Ruddle, 2006). Total HEV surface area, quantified by antibody staining, was noted to increase following immunization (Mebius *et al.*, 1990), with Soderberg (2005) and colleges reporting an increase in HEV number proportional to increase in LN size until at least day four after infection. Additionally, an increase in internal HEV diameter, increasing rapidly after immunization to a peak of 3-times greater at day three, with subsequent decrease to baseline diameter by day twelve with little change to vessel wall thickness (Myking, 1980). This pattern of increasing vascularity soon after infection with eventual resolution in HEVs also holds for studies of general LN vascularity and lymphatic vessels. Tracing of blood-borne microbeads indicate that blood flow to the LN rapidly increases following infection and remains elevated for at least five days, with increased blood flow correlating to increased LN weight. Microangiography also noted increased vascularization within a day of

immunization with a peak at day five that subsequently returned to baseline level (Herman *et al.*, 1972). A similar pattern was seen in the microvasculature of dLNs of skin allographs in which increased vascular permeability is noted as early as twelve hours with peak vascularization around seven days (Anderson *et al.*, 1975). Day seven was also noted as the peak time-point of generalized vascular growth within reactive LNs, as indicated by endothelial cell proliferation, and was linked to DCs by Webster and colleges (2006). Collectively, these past studies of HEVs and general LN vasculature indicate vascular changes throughout the course of infection are dynamic, follow the pattern of adaptive immune on-set and have keys links to the immune response. Therefore, based on the previous findings within the LN in terms of lymph vessels, HEVs, and general vascular growth, the hypothesis that arteriole remodeling would also change throughout the course of infection, peak shortly after the time-point of effector cell migration to the infection site, and then return to baseline was formed. This hypothesis was furthered to include the hypothesis that remodeling of the feed arteriole was an outward euthrophic event, based on studies of HEVs by Myking (1980) and that it would be the most effective remodeled state by which to increase blood supply to the LN and expedite delivery of naïve lymphocytes, as arteriole expansion was shown to facilitate trafficking by Soderberg and colleges (2005).

To address the hypothesis that arteriole remodeling, like HEVs and general vascular growth, correlates to changes in lymph node cellularity and generation of effector cells, IVM experiments aimed at determining the kinetics and magnitude of arteriole remodeling throughout the course of infection were conducted. Results from these experiments were considered in the context of how they correlate to what is know

about the immune response and other vascular changes within the LN. Investigations demonstrate arteriole expansion to commence as early as day one following infection and peak at day seven post infection, following which arteriole diameter returns to pre-infection size. To address the second hypothesis, of outward eutrophic remodeling, H&E stained cross-sections of isolated LN arterioles from multiple time-points after infection were analyzed, with results supporting the hypothesis of outward eutrophic remodeling.

3.2 Results

Bright-field intravital microscopy was used to examine the inguinal LN feed arteriole of C57 BL/6 mice at multiple days after i.vag. infection with Tk$^-$HSV-2. From a baseline average diameter of 85μm at day zero of infection, a significant increase in the resting vessel diameter was notable as early as one day post-immunization (p.i). Resting diameter subsequently continued to increase until seven days p.i., peaking at a average diameter of 165μm. After this peak, the resting diameter declined and returned to a value not different than that seen prior to infection. This was quantified by measurement of the vessels (Figure 3A) and could also be observed via gross examination of equilibrated feed arterioles (Figure 4A).

Maximal vessel diameter was found to have the same temporal pattern of remodeling as resting diameter. Compared to the average baseline diameter at day zero of 117μm, there was a significant increase in maximal diameter by day one p.i. to an average of 142μm. Maximal diameter continued to increase until peaking at seven days p.i. with an average diameter of 187μm before returning to a baseline diameter. As with the resting diameters, these significant increases were notable when comparing measured vessel diameter (Figure 3B) as well as comparison of microscopic images of the feed arteriole vessels following superfusion of the applied vasodilator (Figure 4B). Additionally, the maximal diameter of the feed arteriole returned to the same diameter as that seen prior to infection.

Together, the resting and maximal diameters demonstrate a pattern of increase in vascular supply to the lymph node during infection, which returns to levels seen prior to infection following induction of an adaptive immune response. In both cases, resting and

maximal diameters, maximum vascular growth is seen seven days p.i.. At this point of maximal remodeling, the increase in vascularity represents a 100% increase in resting vessel diameter set-point and a 70% increase in the maximal vessel size when compared to that of an uninfected mouse (Figure 3C).

Figure 3: Wild-Type Lymph Node Arteriole Resting and Maximal Diameters Throughout Infection. A. Resting arteriole diameter at days zero, one, three, five, seven, nine, and thirty-five (5 weeks) after i.vag. infection with TK$^-$HSV-2. **B**. Maximal arteriole diameter at days zero, one, three, five, seven, nine, and thirty-five (5 weeks) after i.vag. infection with TK$^-$HSV-2. Maximal vessel diameters were recorded after superfusion of 100μM SNP. **C.** Resting and maximal vessel size at day seven p.i. relative to day zero p.i. expressed as a percent change. Data represents mean diameter (A,B), and percentage of mean day zero diameter (C) ± SEM wherein n=11, 5, 6, 5, 5, 4, and 4 animals for days 0, 1, 3, 5, 7, 9, and 35 respectively where one arteriole was studied per animal. *$p<0.05$, **$p<0.01$, and ***$p<0.001$.

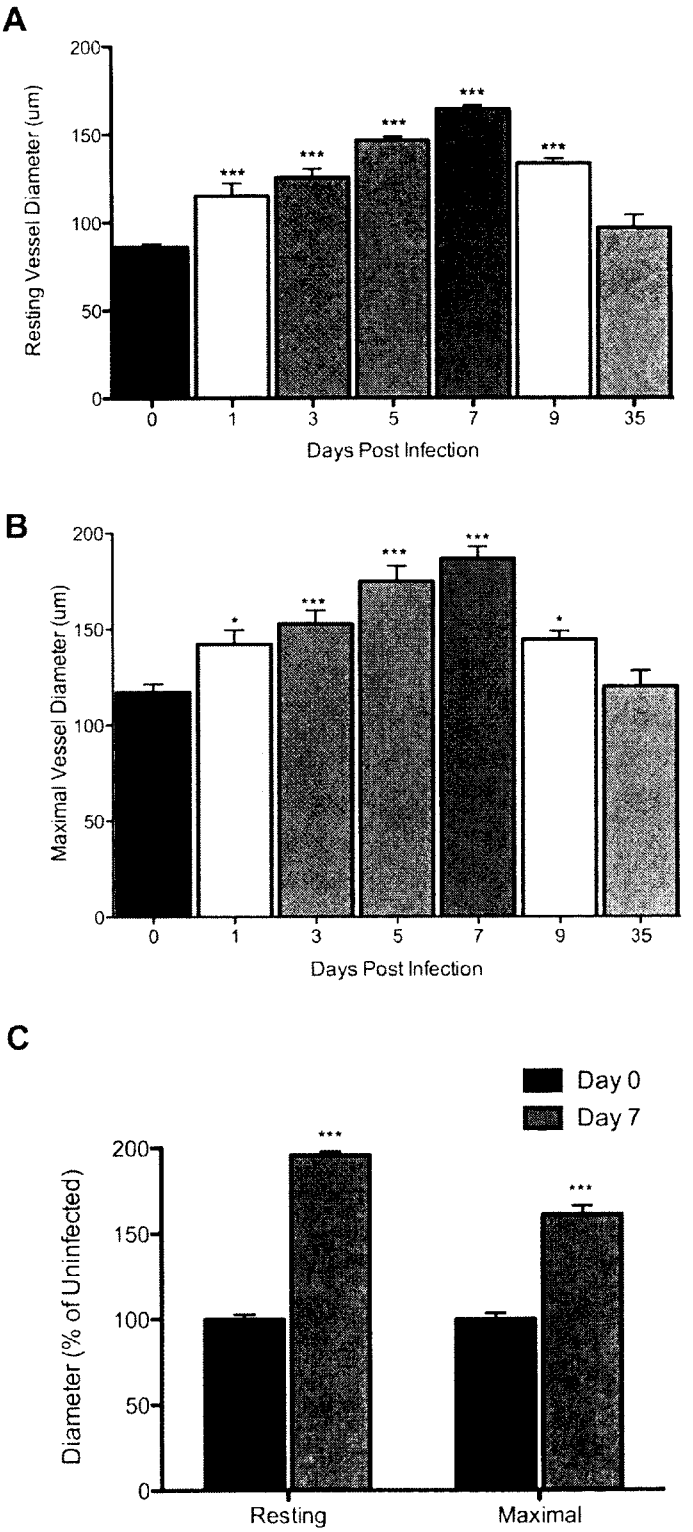
A
Resting Vessel Diameter (um)
200
150
100
50
0
***
0
1
3
5
7
9
35
Days Post Infection
B
Maximal Vessel Diameter (um)
*
Days Post Infection
C
Day 0
Day 7
Diameter (% of Uninfected)
Resting
Maximal

Figure 4: Intravital Microscopy of Wild-Type Lymph Node Arterioles Throughout Infection. A. Representative images of resting diameter arterioles following infection at days zero, three, and seven after infection. **B**. Representative images of maximal diameter arterioles following infection at days zero, three, and seven after infection and application of SNP to the preparation. In all images, the arteriole, which is indicated by green arrows, is shown to the left of the LN venule.

A

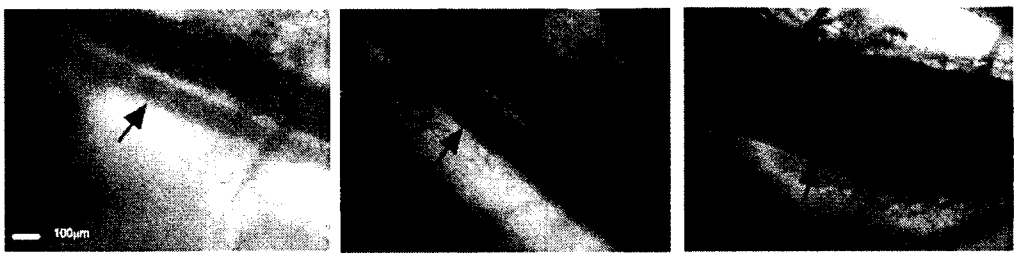

Day 0 Day 3 Day 7

B

Day 0 Day 3 Day 7

At all days post immunization, there is a notable difference in resting and maximal vessel diameters (Figures 3A, B), which demonstrates the ability of the vasculature to respond to an applied vasodilator. This speaks to the health of the studied vessels and the success of the preparation. However, we also wanted to consider the preparation integrity and vasoactive capability of the feed arteriole using phenylephrine (PE), a SMC α_1-adregeneric receptor agonist. A dose response curve from 10^{-9} through to 10^{-5}M PE in physiological saline solution superfused over the preparation was conducted. Uninfected day zero wild-type controls showed dose-dependent vasocontriction; less than one percent constriction was seen at the lowest concentration of 10^{-9}M, but increased significantly, in a dose-dependent manner, and peaked between 50-60% constriction with application of 10^{-5}M PE. Figures 5A and 5B show percent constriction relative to resting diameter and representative images respectively from the dose response curve. Next, to both evaluate the health of the preparations as well as investigate potential changes in smooth muscle response, phenylephrine response curves were conducted at days one, three, five, seven, nine, and thirty-five p.i.. Infected mice at all days showed no significant difference in percent vessel constriction compared to uninfected day zero controls at any concentration of PE (Figure 5C). Therefore, the dose-dependent response to PE and the consistency of the constriction throughout the course of infection support the health of the preparation and indicate that no change is seen in vascular response during infection in wild-type mice.

Figure 5: Wild-Type Lymph Node Arteriole Vascular Response to Phenylephrine During Infection. A. Percent vessel constriction with respect to resting vessel diameter of LN arteriole of wild-type mice at day zero p.i. in response to superfusion PE applied in fold increases from 10^{-9} to 10^{-5}M. **B**. Representative images of lymph node arterioles following at day zero p.i. prior to PE application and following superfusion of 10^{-9}, 10^{-7}, and 10^{-5}M PE. In each image the arteriole is shown to the upper right of the LN venule and indicated by a green arrow. **C**. Percent vessel constriction with respect to resting vessel diameter of LN arteriole of wild-type at day zero, one, three, five, seven, nine, and thirty-five p.i. in response to PE applied in fold increases from 10^{-9} to 10^{-5}M. Data represents percent constriction (A,C) ± SEM were n=6 for day zero and n=5 animals for days one, three, five, seven, nine, and thirty-five where one arteriole was studied per animal. *$p<0.05$, **$p<0.01$, and ***$p<0.001$.

A

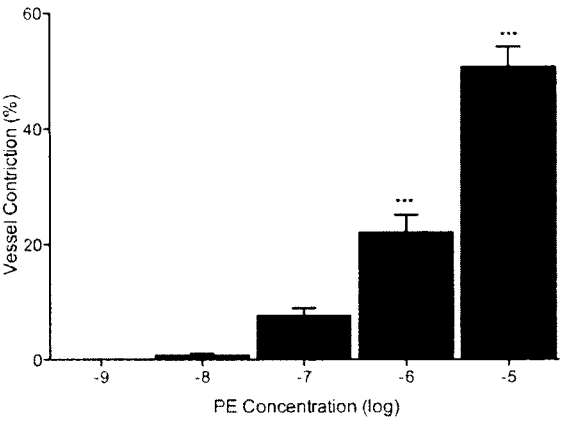

B

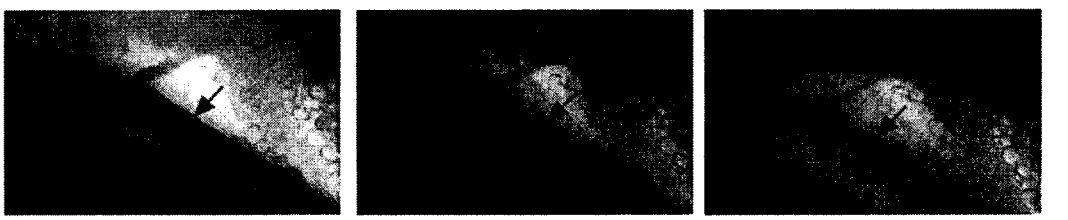

10^{-9}M 10^{-7}M 10^{-5}M

C

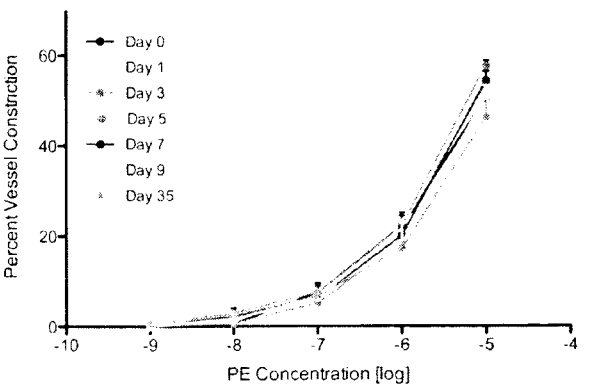

Changes in vessel diameter can occur in a number of ways, such as those discussed above in the introduction, however, given that the blood columns and vessel walls were visible during imaging and the blood columns appeared to be much larger following infection without increase in vessel wall thickness (Figure 4). These findings subsequently lead to the hypothesis that the arteriole expanded by outward remodeling without any neointimal formation. To address this hypothesis, cross-sections from days zero, seven, and thirty-five were H&E stained (Figure 6). All stained sections showed similar wall thickness throughout the course of infection, thereby supporting outward eutrophic arteriole remodeling.

Figure 6. H&E Staining of Wild-Type Lymph Node Arteriole Sections During Infection. LN arterioles treated with 100μM SNP and isolated from anesthetized mice and then fixed in 10% buffered formalin and then embedded in paraffin. Sections were H&E stained and imaged at 400x using a standard light microscope. Representative images are shown for days zero, seven, and thirty-five following infection, where the vessel wall is indicated by the blue arrow and the adventitia is indicated by the red arrow.

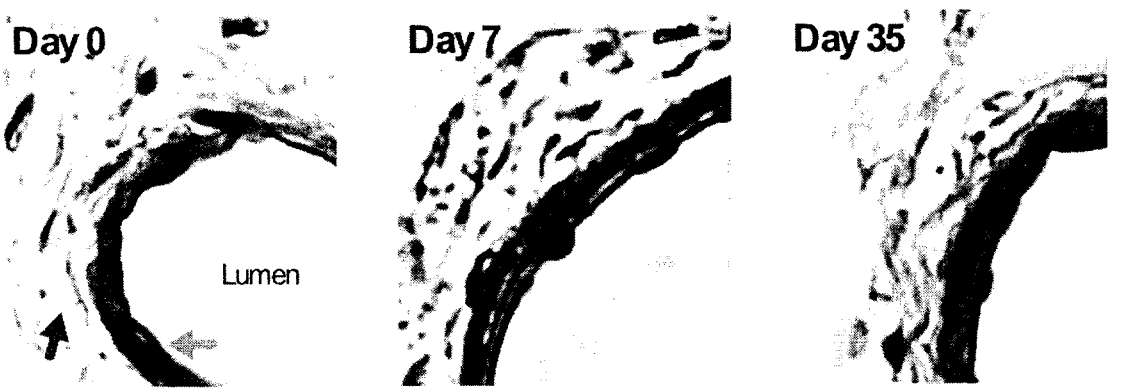
Day 0
Lumen
Day 7
Day 35

3.3 Discussion

These experiments are the first to demonstrate and characterize reversible remodeling of the LN feed arteriole during infection. These findings show that remodeling is first notable day one p.i., and that expansion continues until day seven p.i. following which diameter begins to return to a size similar to that seen prior to infection. The complete characterization of the kinetics and magnitude of arterial remodeling is vital; it allows for connections to be made between changes to the feed arteriole and other events within the lymph node. The timeline of remodeling, being noted as early as day one p.i., and continuing until day seven p.i., supports the hypothesis that arteriole remodeling aids the induction of adaptive immune response as the process of remodeling mirrors the timeline of adaptive immune response (Murphy *et al.*, 2008) including the generation of antigen specific effector cells (Nakanishi *et al.*, 2009) and the mechanism of facilitating T cell migration to the lymph node as cellular accumulation within the node as well as rate of lymphocyte accumulation and organ hypertrophy has been shown to increase soon after immunization with Tk$^-$HSV-2 and continue until at least day five p.i. (Soderberg *et al.*, 2005).

Beyond corresponding to the timeline of immune response, arteriole remodeling also resembles other patterns of vascular growth noted within the LN including generalized growth and changes in HEVs. Reactive HEVs have been shown to have a spike in internal diameter that starts within a day, spikes, and returns to baseline around twelve days following stimulation (Myking, 1980), while other studies demonstrate HEV numbers to increase proportional to LN size until at least day four following infection with HSV-2 (Soderberg *et al.*, 2005). Stimulation with oxazolone, an immunological

adjuvant commonly used to induced hypersensitivity reactions, also resulted in increased HEV area spiking around day four before returning to baseline (Mebius *et al.*, 1990). Additionally, early studies show increased capillary diameter and density within twenty-four hours following stimulation, increasing through day five followed by return to pre-stimulated state (Herman *et al.*, 1972). Furthermore, Hays & Hobbs (1977), based on microsphere accumulation and cardiac output, suggest that increased blood flow to draining lymph nodes is the result of hyperemia for the first twenty-four hours and subsequently the result of vascular growth over the course of more than four days. Therefore, comparing new findings presented here to the time-course of immune response seen during HSV-2 infection, and previously noted kinetics of HEV and LN vascular changes during immune response, implies that the mechanism of arteriole remodeling is induced by cells that migrate early during infection or are resident in the lymph node and that the mechanism governing HEV expansion and proliferation may also be key in facilitating arteriole expansion.

The mechanism of arteriole remodeling was partially indicated by H&E staining of arteriole cross-sections shown above. The finding of reversible outward euthrophic remodeling was exciting, as although changes in vascularity have been shown to occur in other vascular beds during infection, in all cases this is pathogenic and irreversible. For example in chronic inflammation, which can be the precursor to many diseases such as airway disease, where arterioles, capillaries and venules are all pathogenically and chronically enlarged (Ezaki *et al.*, 2001) or in pulmonary arterial remodeling in response to hypertension (Daley *et al.*, 2008). In contrast, remodeling of the LN arteriole is not, as highlighted by the return of vessel diameter to baseline that coincides with the clearance

of infection. This also partitions arteriole remodeling into two distinct phenomenon: expansion and reversion to homeostatic size. The first phase, expansion, which was shown to occur via outward eutrophic remodeling, may first involve hyperemia with subsequent vascular growth. Hays & Hobbs (1977) first proposed this model within the lymph node based on two distinct spikes in LN blood flow, the first is noted as early as one and a half hours after stimulation and peaks around fourteen hours and the second begins around day two p.i. and continues past day four p.i. and was based on the kinetics of endothelial cell division. The concept of early hyperemia is also supported by data that will be detailed in subsequent chapters that reveal a role of inflammatory mediators within the LN feed arteriole and shifts in resting arteriole diameter. Vascular expansion following initial hyperemia is further supported by studies that show ECs numbers to increase in the LN by day three and peak at day seven following stimulation. However, BrdU was incorporated in the LN within the first twenty-four hours and increased through to day five, indicating the events of EC proliferation in the LN occurs early after stimulation and increases in correspondence with the timeline seen here in arteriole remodeling. Interestingly, the same study subsequently demonstrated EC proliferation to be dependent upon dendritic cells, L-selectin, and VEGF, all of which will be considered and discussed in subsequent chapters (Webster *et al.*, 2006). Additionally, and notably, ECs proliferation within the stimulated LNs was also shown to be present in both $PNAd^+$ (eg. HEVs) and $PNAd^-$ (eg. arteriole, lymphatics) cells within the LN, which supports the potential for ECs proliferation within the LN arteriole during remodeling (Chyou *et al.*, 2008).

Kinetics of endothelial cell division and vascular changes in non-LN settings also correspond to the current findings within the LN feed arteriole. For example, in the context of infection leading to inflammatory airway disease, increased arteriole diameters peaked seven days following infection and was accompanied by increased EC proliferation indicated by BrdU incorporation which peaked five days after infection and stopped at day nine (Daley *et al.*, 2008, Ezaki *et al.*, 2001). Similar patterns are also seen in angiogenesis where proliferation has been shown to peak around day three and persist through day six in the context of both graft-versus host and hypersensitivity type immune responses (Polverini *et al.*, 1977, Sidky *et al.*, 1975). Beyond endothelial cell proliferation, EC hypertrophy as also been noted in HEVs following stimulation, which subsequently returned to baseline (Myking, 1980) and is also an indicator or rapid EC proliferation (Ezaki *et al.*, 2001). Therefore, a general conclusion that the dynamics of EC proliferation and hypertrophy, as noted within the LN and in other non-LN environments, corresponds to the timeline of arteriole remodeling within the LN can be drawn. This is an important conclusion as outward eutrophic remodeling, as is observed in the LN arteriole, would require increased EC size or number. As such, this supports the future hypothesis that LN arteriole remodeling is driven by EC proliferation, hypertrophy and/or recruitment.

The second part of the arteriole phenomenon, return to baseline diameter, is just as interesting as the expansion of the arteriole, because while understanding how to induce and augment or inhibit remodeling would allow for control of on-set of adaptive immunity, learning how the process is reversed would provide new therapeutic insight; in most cases of outward vessel remodeling, including inflammatory airway disease and

pulmonary hypertension (Daley *et al.*, 2008, Ezaki *et al.*, 2001) the event is a largely permanent process and associated with vascular dysfunction and disease progression. Therefore, understanding how arteriole remodeling within the LN is reversible, may allow us to generate new theories on how to reverse pathological forms of remodeling. However, while the potential mechanism driving arteriole expansion will begin to be addressed in subsequent chapters of this thesis, how expansion occurs with subsequent return to baseline occurs is a planned future direction. As the current hypothesis proposed was that expansion may occur through a combination of hyperemia, and endothelial cell proliferation, but studies to address these possibilities have yet to be completed, the exploration of mechanism of the LN arteriole return to baseline diameter first requires confirmation of the mechanism of expansion. As such, this will be addressed in the future directions section of the final chapter along with other factors that are important future considerations such as shear stress levels, blood flow rate, effect of different pathogens, and impact on adhesion molecules which will further add to the novel and notable findings of the extent and timeline of reversible arteriole remodeling of the inguinal LN feed arteriole following HSV-2 infection.

CHAPTER FOUR – $CD4^+$ T-Cells in Lymph Node Arteriole Remodeling

4.1 Introduction

Having established the kinetics and magnitude of lymph node arteriole remodeling, coupled with its importance in facilitating cellular accumulation within reactive LNs (Soderberg *et al.*, 2005), understanding how remodeling is initiated and maintained in the first place is important because facilitating faster and/or increased entry into lymph nodes would serve to decrease the duration of the rate limiting process of screening for cognate lymphocytes. In generating hypotheses for the mechanism governing remodeling of the LN feed arteriole, supporting evidence is derived from two general sources. First, studies looking at generalized vascular growth as well as HEV and lymphatic growth in LN during immunization, and second, studies discerning the mechanism of eutrophic outward remodeling. Here, we will focus on consideration of the first, studies looking at LN vascular growth.

Studies of LN vascular growth are numerous. However, what is known about vascular remodeling within the lymph node is largely limited to the study of HEVs and generalized vascular growth. These studies highlight the mechanism of vascular growth within the LN and at the HEV level to be dependent upon dendritic cells regulating VEGF levels (Webster *et al.*, 2006) potentially mediated through the FRC network (Chyou *et al.*, 2008) and B cells involving LTβR cross-talk (Angell *et al.*, 2006). However, when considering these studies for indication of the possible mechanism of arteriole remodeling, it is notable that HEVs have a distinct phenotypes (von Andrian & Mempel, 2003). This presents the possibility that the mechanism of remodeling of the LN arteriole may be different than those mechanisms implicated downstream of the arteriole.

Additionally, given that the feed arteriole is directly upstream of and feeds HEVs, the mechanism of arteriole remodeling may directly or indirectly drive changes in HEV phenotype and function during infection. For example, increased blood flow from arteriole remodeling could alter shear stress levels, distribution of blood borne chemokines and inflammatory mediators, and migration of immune cells all of which would act upon the HEV. Notably, the reverse theory is also a possibility; signaling and mediators of vascular growth may be transmitted upstream from the LN and/or HEVs to act upon the feed arteriole such as has been seen with VEGF secretion within the LN that subsequently acts upstream on the HEVs (Webster *et al.*, 2006). However, determining the impact of arteriole remodeling on HEVs or vice versa and subsequent impact on cellular trafficking and induction of a robust adaptive immune response first requires uncoupling different levels of vascular growth of the LN (ie. LN cortex, HEVs, arteriole), which, in turn, requires first determining the specific mechanism driving LN arteriole remodeling and underscores the importance of the aim of this section of the study: to begin to elucidate mechanism of LN arteriole remodeling during infection.

Despite the differences between HEVs and LN vasculature and the LN arteriole itself and no indication if changes in one (LN vasculature/HEV or arteriole) affects the other, this is the most relevant source upon which to base a hypothesis on the mechanism of arteriole remodeling given the paucity of information on the LN arteriole. Therefore, based on findings that indicate DCs, acting through VEGF, as key components in EC proliferation within draining LNs as well as HEV phenotypes, an original working hypothesis that DCs are a critical factor in LN arteriole remodeling was formed. However, the approach to examine this hypothesis was to determine the role of $CD4^+$ T

cells. This investigative plan was based on the fact that during induction of adaptive immune response naïve $CD4^+$ T cells amass in the draining LN via movement through the LN feed arteriole and trafficking through the HEVs that are fed by the arteriole. This gives the large number of $CD4^+$ T cell moving through the arteriole access to directly or indirectly act upon the feed arteriole. Notably, T cells have been implicated in other forms of arteriole remodeling (Daley *et al.*, 2008) and vascular adaptation (Burne *et al.*, 2001), including induction of arteriogenesis (Stabile *et al.*, 2003). Furthermore, investigating the role of $CD4^+$ T cells would indirectly indicate a role of DCs, due to their extensive interaction in the LN, while at the same time potentially identifying a novel role of $CD4^+$ T cells in vascular growth. Therefore, a new hypothesis, that $CD4^+$ T cells drive LN arteriole remodeling, was formed prompted by consideration of the extensive interactions that occur between DCs and $CD4^+$ T cells in the reactive LN, the central role of $CD4^+$ T cells in adaptive immunity on-set and LN hypertrophy, and evidence of $CD4^+$ T cell involvement in other forms of remodeling.

Investigation of $CD4^+$ T cells is most strongly supported by its diverse and vital interactions and roles in the LN; during infection, LN are the main site of screening for antigen specific $CD4^+$ T cells and subsequent T cell priming. This first involves entry of naïve $CD4^+$ T cells into the LN, which is dependent upon induction of T cell rolling along the HEV via L-selectin (CD62L) expressed on the T cell binding to peripheral node addressin on the HEV luminal surface. Specifically, L-selectin binds the sulfated sialyl-$Lewis^x$ carbohydrate moiety of CD34 and GlyCAM-1. Subsequently, activation of the rolling T cell is induced by interaction of CCR7 with CCL21 and CCL19 and CXC12 with CXCR4. Finally, arrest is mediated by the binding of LFA-1 to ICAMS on the HEV

(Ley *et al.*, 2007, Miyasaka & Tanaka, 2004, Murphy *et al.*, 2008, von Andrian & Mempel, 2003). Notably, in addition to this complex trafficking cascade, remodeling of the LN feed arteriole aids lymphocyte recruitment to the LN, and activation of toll-like receptors alone is sufficient to induce cellular accumulation and LN hypertrophy (Soderberg *et al.*, 2005). Collectively, this speaks to the trafficking of T cell to LNs as a diverse interaction of the vasculature at both the arteriole and HEV level as well as immune signaling at the site of infection and within the LN.

Once in the lymph node, $CD4^+$ T cells transiently interact with antigen presenting cells in the T cell zones in the process of screening for rare cognate lymphocytes. This interface is facilitated by interaction of CD2, LFA-1 and ICAM-3 on the T cell with CD58, ICAM-1 & 2, and DC-SIGN respectively on dendritic cells. When a naïve T cell is identified that corresponds to the peptide-MHC complex being presented by the DC, a conformational change occurs in LFA-1 as a result of signaling through the T cell receptor (TCR), which stabilizes the T cell to DC interaction. Subsequent co-stimulation of the T cell via interaction of CD28 on the T cell with B7 molecules on the DC provides survival signals. DCs, as well as cytokines such as IL-2, IL-6, and IL-12, also regulate T cell differentiation. In the late stage of proliferation, activated T cells acquire effector functions, of which there are a number of categories. The two main forms of $CD4^+$ T cells are termed T_H1 and T_H2 cells and are frequently referred to as helper T cells due to their role in aiding other components of the immune system. T_H1 cell enhance the microbial properties of macrophages. Meanwhile, T_H2 are noted in aiding B cell activation; B cell activation by T_H2 is mediated through CD40 interaction with CD40 ligand (CD40L), which results in cytokine production by the T_H2 cell to activate the B

cell (Abbas *et al.*, 1996, Bromley *et al.*, 2001, Kapsenberg, 2003, Murphy *et al.*, 2008, von Andrian & Mempel, 2003).

$CD4^+$ T cells also have an impact on the induction of antigen specific $CD8^+$ T cell or cytotoxic T lymphocyte (CTL) responses in the LN. CTLs are critical to fighting intracellular pathogens as they recognize viral peptides displayed by infected cells on MHC class I complexes and subsequently kill the infected cells. Cell death is achieved through the release of cytotoxic granules containing perforin, granyzme, and granulysin (Murphy *et al.*, 2008, Barry & Bleackley, 2002). Notably, the ability to produce granzyme, as well as the expression of CD69 can be used for evaluation of CTL effector responses (Kumamoto *et al.*, 2011). The production of active CTLs is also another instance in which CD4 influence/interaction with DCs is critical; within the LN, $CD4^+$ T cells aid CTL responses in multiple ways including licensing of dendritic cells (DCs) for efficient antigen presentation as DCs activated by $CD4^+$ T cells are able to more efficiently prime cognate $CD8^+$ T cells through the expression of CD25, the alpha chain of the interleukin 2 (IL-2) receptor which increases binding of affinity of IL-2 which drives T cell proliferation, and CD127, the interleukin 7 receptor which plays a role in maintaining secondary responses. Furthermore, antigen specific $CD4^+$ T cells facilitate the recruitment of naïve $CD8^+$ T cell via secretion of CCL3 and CCL4, thereby increasing the efficiency of producing memory CTLs (Behren *et al.*, 2004, Castellino & Germain, 2006, Murphy *et al.*, 2008, Smith *et al.*, 2004). In the instance of HSV-2 infection, CTL responses are robust (Kolle *et al.*, 1998) and $CD4^+$ T cells are required for the generation of both primary and secondary CTLs (Janssen *et al.*, 2003, Kumamoto *et al.*, 2011, Rajasagi *et al.*, 2009).

The link between arteriole remodeling and adaptive immunity on-set (Soderberg *et al.*, 2005) speaks to the great importance of determining the mechanism of remodeling, and all of the major points noted above support the investigation of $CD4^+$ T cells as a driving force in LN arteriole remodeling. To this end, experiments detailed below dissect the role of $CD4^+$ T cells in LN arteriole remodeling following HSV-2 infection, and demonstrate it to be $CD4^+$ T cells dependent. Furthermore, in combination with excellent work by collaborators in Dr. Iwasaki's lab at Yale University the conclusion that arteriole remodeling dependence on $CD4^+$ T cells is driven by $CD4^+$ T cell interaction with DCs through MHC II to TCR and through CD40 and CD40L interface is drawn and Dr. Iwasaki's groups further shows that this was a critical factor in facilitating naïve polyclonal $CD8^+$ T cells entry into the LN, which resulted in decreased magnitude of CTL response to infectious agent (Kumamoto *et al.*, 2011) and identifies $CD4^+$ T cell driven vascular growth of the LN feed arteriole as a mediator of CTL responses.

4.2 Results

To determine if $CD4^+$ T cell were required for lymph node arteriole remodeling, LN feed arterioles in mice deficient in $CD4^+$ T cells due to genetic ablation ($CD4^{-/-}$ mice), which have not previously been noted to have defects in LN vasculature, following infection with Tk$^-$HSV-2 were examined. Arterioles in these mice showed no significant difference in resting vessel diameter at one, three or seven days after infection when compared to day zero controls (Figure 7A). The extent to which remodeling is inhibited is most blatant when comparing arterioles from day zero p.i. and day seven p.i. in $CD4^{-/-}$ mice to each other as well as to an arteriole from a day seven p.i. WT C57 BL/6 mouse, which is notably larger on gross examination (Figure 7B), as well as when comparing the increase in resting diameter at days three and seven p.i. relative to the mean diameter at day zero p.i. (Figure 7C). This data indicates that $CD4^+$ T cells are required to regulate a change in resting LN arteriole set-point during induction of adaptive immune response as in the absence of $CD4^+$ T cells there is no notable increase in resting arteriole diameter following infection as is seen in wild-type mice.

As the mechanism governing resting arteriole tone and therefore set-point, may be different than that governing remodeling and maximal vessel diameter, maximal vessel diameter was also examined. Similar to resting vessel diameter, maximal vessel diameter remained unchanged at days zero, three, and seven p.i. in comparison to day zero controls. Day zero controls had an average maximal vessel diameter of 144μm in comparison to average diameters of 142, 131, and 129μm at days one, three, and seven p.i. respectively (Figure 8A). This lack of LN arteriole remodeling is in distinct contrast to maximal vessel remodeling observed in day seven p.i. WT arterioles (Figure 8B) and is

characterized by significantly decreased levels of arteriole expansion, relative to uninfected day zero controls, when compared to WT mice (Figure 8C). Given that WT mice were infected throughout the course of the study and consistently demonstrated LN arteriole remodeling and $CD4^{-/-}$ mice showed characteristic signs of infection including redness and lesions around the infection site which indicates successful infection, these findings show that $CD4^{+}$ T cells are required for expansion of the draining lymph node feed arteriole throughout the course of infection.

Figure 7: $CD4^{-/-}$ Lymph Node Arteriole Resting Vascular Profile Throughout Infection. A. Resting arteriole diameter at days zero, one, three, and seven after i.vag. infection with TK^{-}HSV-2 of $CD4^{-/-}$ mice. **B**. Representative images of resting diameter arterioles following infection at days zero, and seven after infection from $CD4^{-/-}$ mice in comparison to maximal remodeling noted at day seven in C57 BL/6 (WT) mice. In each image a green arrow indicates the arteriole. **C.** Resting vessel size at day one, three, and seven p.i. relative to mean day zero p.i. diameter expressed as a percent change for WT and $CD4^{-/-}$ mice. Data represents mean diameter (A) or percentage of day zero diameter (C) ± SEM wherein n=4 for day zero and n=5 for each of day one, three, and seven in $CD4^{-/-}$ mice and n=11, 6, and 5 for WT mice at days zero, three, and seven p.i. respectively with one arteriole studied per animal. *$p<0.05$, **$p<0.01$, and ***$p<0.001$.

A

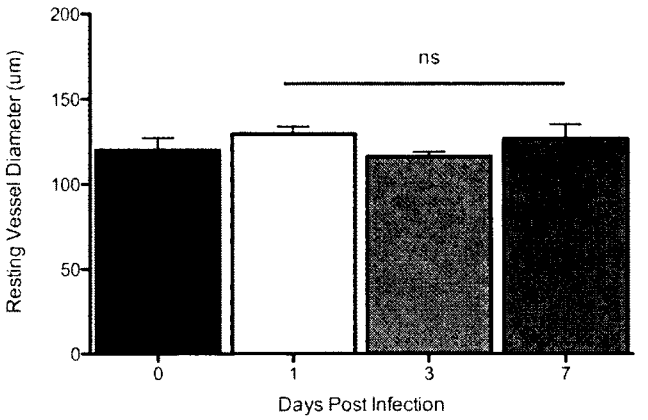

B

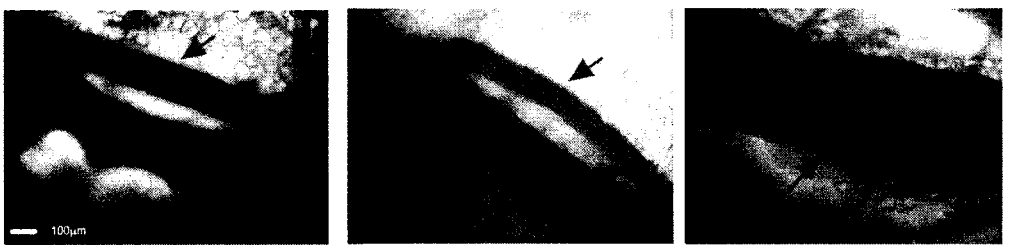

CD4$^{-/-}$ Day 0 CD4$^{-/-}$ Day 7 WT Day 7

C

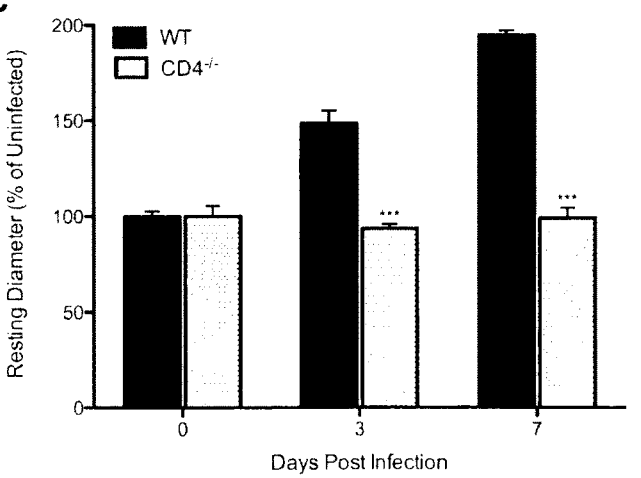

Figure 8: $CD4^{-/-}$ Lymph Node Arteriole Maximal Diameter Vascular Profile Throughout Infection. A. Maximal arteriole diameter at days zero, one, three, and seven after i.vag. infection with TK^{-}HSV-2 of $CD4^{-/-}$ mice. Maximal vessel diameters were recorded after superfusion of 100μM SNP. **B**. Representative images of maximal diameter arterioles following infection at days zero, and seven after infection from $CD4^{-/-}$ mice in comparison to maximal remodeling noted at day seven in C57 BL/6 (WT) mice. In each image a green arrow indicates the arteriole. **C.** Maximal vessel size at day one, three, and seven p.i. relative to mean day zero p.i. diameter expressed as a percent change for WT and $CD4^{-/-}$ mice. Data represents mean diameter (A) or percentage of day zero diameter (C) ± SEM wherein n=4 for day zero and n=5 for each of day one, three, and seven in $CD4^{-/-}$ mice and n=11, 6, and 5 for WT mice at days zero, three, and seven p.i. respectively with one arteriole studied per animal. *p<0.05, **p<0.01, and ***p<0.001

A

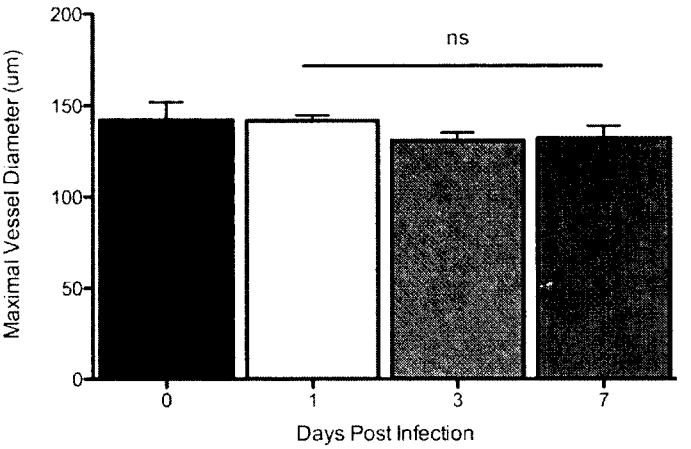
200
150
100
50
0
Maximal Vessel Diameter (um)
ns
0
1
3
7
Days Post Infection

B

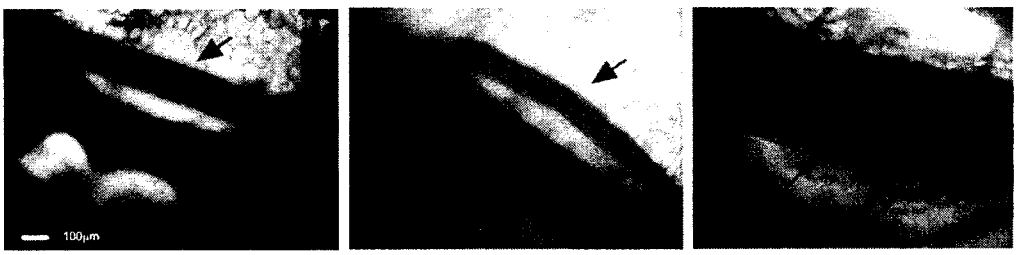
100µm
CD4-/- Day 0
CD4-/- Day 7
WT Day 7

C

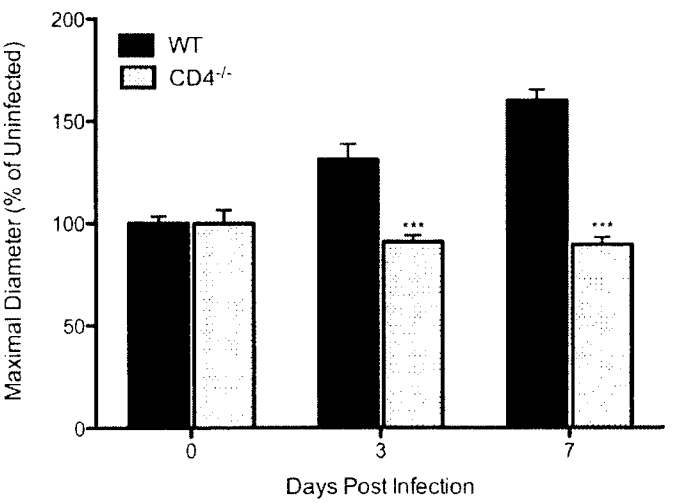
200
150
100
50
0
Maximal Diameter (% of Uninfected)
WT
CD4-/-
***
***
0
3
7
Days Post Infection

In addition to determining resting and maximal vessel diameters, vasoconstriction in response to phenylephrine was evaluated to assess preparation health as well as any change in smooth muscle function that may result from the absence of $CD4^+$ T cells (Figure 9A) as $CD4^+$ T cells have been shown to induce increased smooth muscle density in pulmonary arterioles (Delay *et al.*, 2008) and induce vascular damage (Burne *et al.*, 2001, Cuttica *et al.*, 2010). Furthermore, cross sectioning and H&E staining of LN arterioles were obtained (Figure 9B). $CD4^{-/-}$ arterioles at all days following infection, including day zero controls, showed constriction in response to phenylephrine similar to that seen in WT controls and H&E staining showed no change in arteriole morphology compared to WT controls as well as consistent morphology throughout the course of infection.

Next, the potential to inhibit remodeling pharmacologically by using mice depleted of $CD4^+$ T cells via antibody treatment was explored. Mice depleted of $CD4^+$ T cells showed no increase in resting or maximal vessel diameter three or seven days post-immunization (Figure 10A, B) with response to phenylephrine consistent to that seen in WT mice (Figure 10C). Notably, while day zero controls were given antibody and a separate set of vehicle (sterile PBS) treated mice were not tested, this is a well established model in Dr. Iwasaki's lab and depleted mice at day zero p.i. had similar resting and maximal arteriole diameters to WT mice (Figure 10D). Together, these results show that pharmacological inhibition of arteriole remodeling is possible through antibody depletion of $CD4^+$ T cells and support conclusions from $CD4^{-/-}$ mice that LN arteriole remodeling during infection is dependent upon $CD4^+$ T cells.

As the requirement for $CD4^+$ T cells was supported in both genetic ablation and pharmacological inhibition, experiments subsequently aimed to determine if $CD4^+$ T cells were required within the lymph node or were capable of supporting arteriole expansion from the periphery. To test this, arteriole remodeling in L-selectin$^{-/-}$, a key selectin in naïve $CD4^+$ T cell migration to LNs during infection (Finger *et al.*, 1996), was explored. Preliminary vessel size data and images are shown and suggests that genetic ablation of L-selectin inhibits lymph node arteriole remodeling (Figure 11A, B), which would indicate that the requirement for $CD4^+$ T cells in the LN arteriole expansion is in the LN itself and $CD4^+$ T cells in the periphery are not sufficient to drive remodeling. However, unfortunately, an inability to access more L-selectin$^{-/-}$ mice prevented completion of this data set.

Figure 9: $CD4^{-/-}$ Arteriole Phenylephrine Response and H&E Staining of Node Arteriole Sections During Infection. LN arterioles treated with 100μM SNP and isolated from anesthetized mice and then fixed in 10% buffered formalin and then embedded in paraffin. Sections were H&E stained and imaged at 400x using a standard light microscope. Representative images are shown for **A**. day zero p.i. **B**. day seven p.i..

A

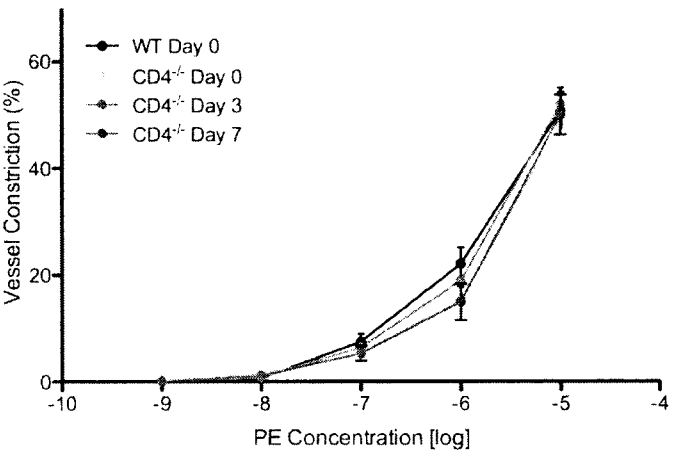

B

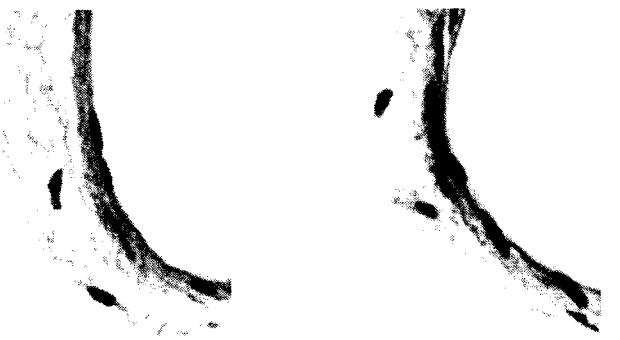

CD4-/- Day 0 CD4-/- Day 7

Figure 10: Arteriole Remodeling in $CD4^+$ T Cell Depleted Mice. A. Resting arteriole diameter zero, three, and seven days after i.vag. infection in CD4 depleted mice. **B**. Maximal arteriole diameter (+100μM SNP) zero, three, and seven days after i.vag. infection. **C**. LN arteriole phenylephrine (PE) dose response from 10^{-9}M to 10^{-5}M at zero, three, and seven days post-infection. **D.** Resting and maximal diameters of WT mice and CD4 depleted mice at day zero. Data represents mean diameter (A, B, D) and mean vessel constriction (C) ± SEM. *p<0.05, **p<0.01, ***p<0.001, ns=no significant difference. N=3, 5, and 4 for days zero, three, and seven p.i. respectively in CD4 depleted mice and n=11 for WT mice at day zero p.i. with one arteriole studied per animal.

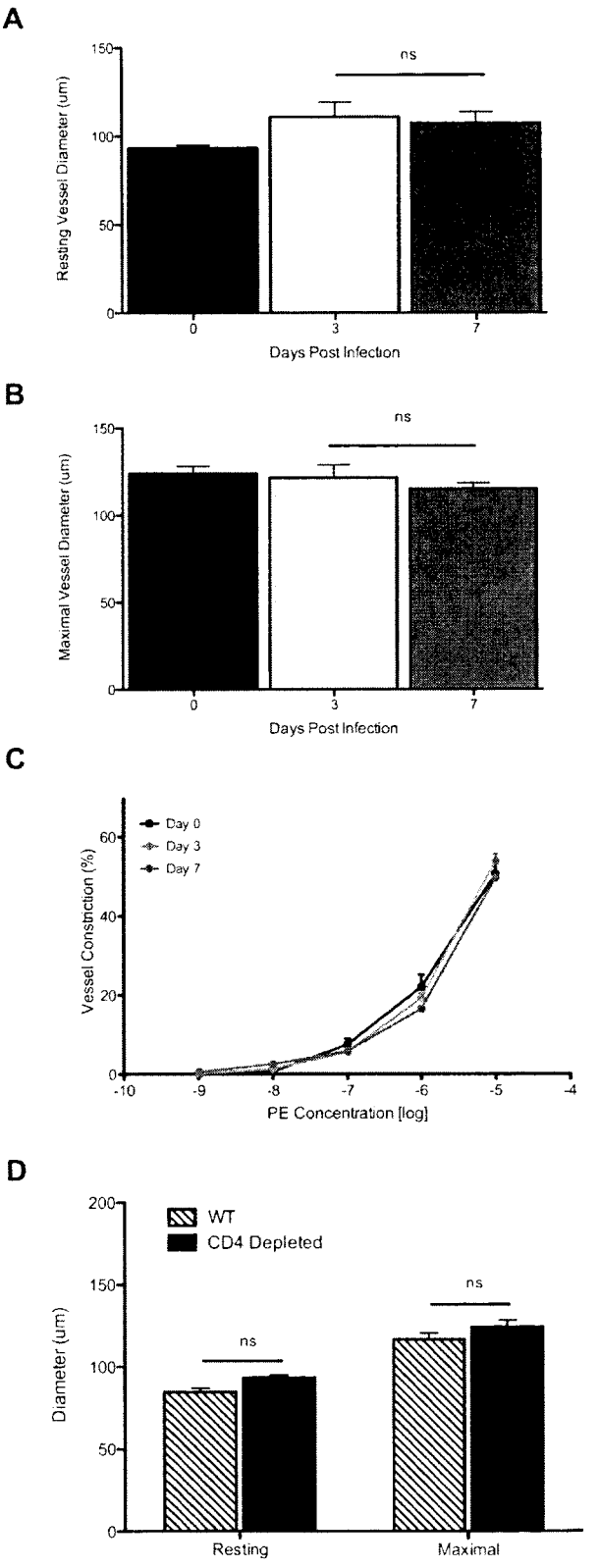
A
Resting Vessel Diameter (um)
150
100
50
0
ns
0
3
7
Days Post Infection
B
Maximal Vessel Diameter (um)
150
100
50
0
ns
0
3
7
Days Post Infection
C
Vessel Constriction (%)
60
40
20
0
Day 0
Day 3
Day 7
-10
-9
-8
-7
-6
-5
-4
PE Concentration [log]
D
Diameter (um)
200
150
100
50
0
WT
CD4 Depleted
ns
ns
Resting
Maximal

Figure 11: Arteriole Remodeling in L-selectin$^{-/-}$ Mice. A. Resting and maximal vessel diameters in L-selectin$^{-/-}$ at days at zero and seven days following infection with Tk^{-}HSV-2. **B.** Representative images of resting L-selectin$^{-/-}$ lymph node feed arterioles at days zero and seven p.i.. where n=1 for all points.

A

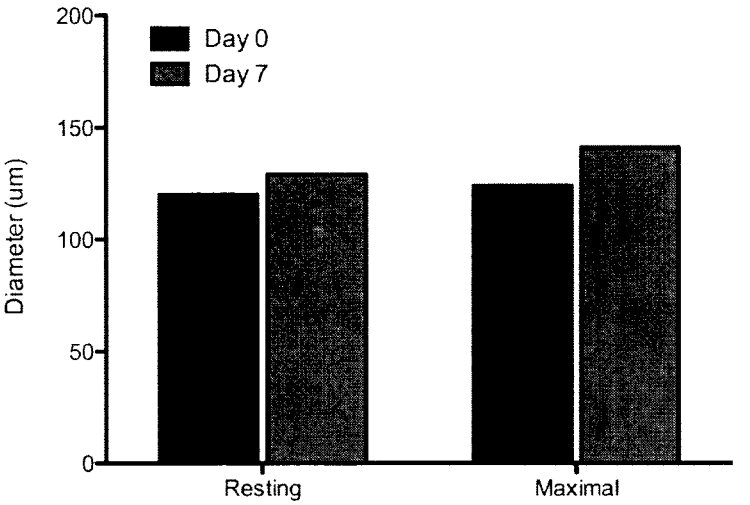

B

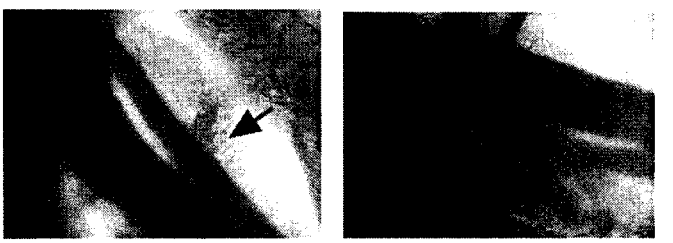

Day 0 Day 7

Given the dependence of LN arteriole remodeling on the presence of $CD4^+$ T cells, disease processes that decreased circulating levels of $CD4^+$ T cells may also inhibit arteriole remodeling. To explore this possibility, arteriole remodeling in aged mice was looked at because aging of the immune system is characterized by a decrease in the number of circulating naïve $CD4^+$ T cells. Interestingly, aged mice showed no increase in resting or maximal vessel diameter seven days p.i. when compared to day zero controls (Figure 12A). Additionally, comparing the relative increase in resting and maximal vessel diameter at day seven clearly demonstrates lymph node arteriole remodeling is significantly inhibited in aged mice, which had an average age of 22 months, in comparison to adult mice, which ranged from 8 to 20 weeks of age (Figure 12B). Finally, although old mice at day zero p.i., had phenylephrine response curves similar to adult mice, response to PE were consistently and significantly blunted at 10^{-6}M and 10^{-5}M concentrations seven days following infection (Figure 12C), indicating a change in arteriole physiology during infection in aged mice that is not seen in adults.

Figure 12: Arteriole Remodeling in Old Mice. A. Resting and maximal (+100μM SNP) arteriole diameter zero and seven days after i.vag. infection in aged mice (average age= 22 months) where n=4 for day zero and n=6 for day seven. **B**. Vessel size at day seven p.i. relative to uninfected day zero mice in adult and old mice. Comparison is expressed as a percent increase over day zero controls to normalize for increased arteriole size seen in larger, older mice. **C**. Phenylephrine (PE) dose response (percent vessel constriction) from 10^{-9}M to 10^{-5}M at zero and seven days p.i.in old mice where n=4 and 6 respecitvely in comparison to days zero and seven in adult mice where n=6 and 5 respectively. Data represents mean diameter (A), mean diameter expressed as a percentage of day zero controls (B), and mean vessel constriction (C) ± SEM where one arteriole was studied per mouse. *$p<0.05$, **$p<0.01$, ***$p<0.001$.

A

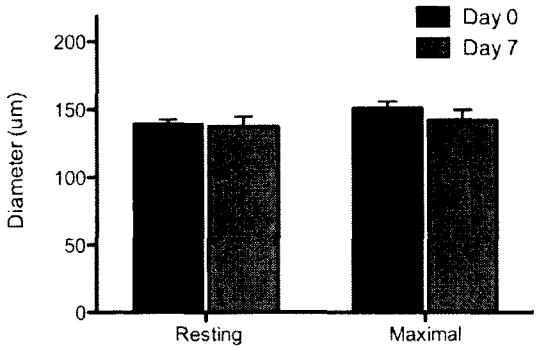
Day 0
Day 7
Diameter (um)
200
150
100
50
0
Resting
Maximal

B

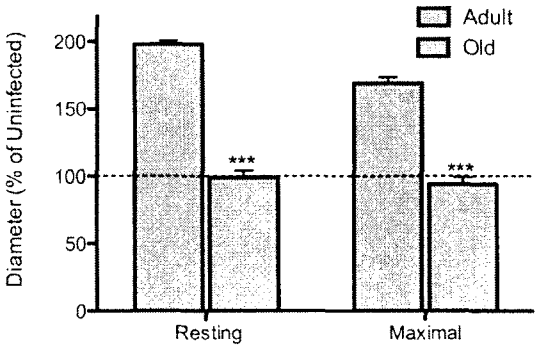
Adult
Old
Diameter (% of Uninfected)
200
150
100
50
0
***
***
Resting
Maximal

C

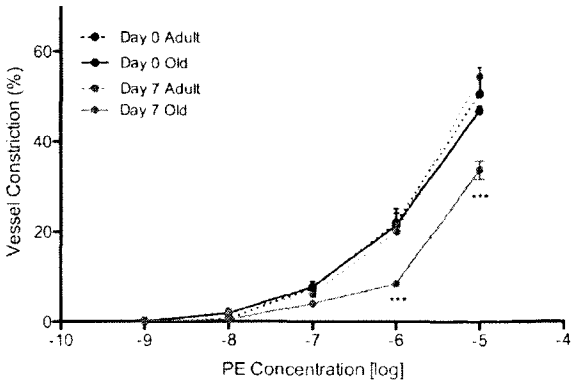
Day 0 Adult
Day 0 Old
Day 7 Adult
Day 7 Old
Vessel Constriction (%)
60
40
20
0
***
***
-10
-9
-8
-7
-6
-5
-4
PE Concentration [log]

4.3 Discussion

Here, the first step in determining the mechanism of LN feed arteriole remodeling is provided by demonstrating that the process is $CD4^+$ T cell dependent, which represents a notable step forward in the current understanding of LN vascular regulation. Interestingly, $CD4^{-/-}$ mice had larger diameter LN arterioles than wild-type mice in the uninfected state, indicating that $CD4^+$ T cells may play a role in not only regulating LN vasculature during infection, but also during homeostasis. This suggests that $CD4^+$ T cells may play a role in regulating the steady-state (Kumamoto *et al.*, 2011). Despite this difference in wild-type and $CD4^{-/-}$ vessel size, the conclusion that $CD4^+$ T cells are required for LN arteriole remodeling is confirmed by studies showing inhibition of remodeling in wild-type (C57 BL/6) mice depleted of $CD4^+$ T cells, because it demonstrates the inhibitory effect of loss of $CD4^+$ T cells in a strain in which LN arteriole remodeling is known to be robust. Furthermore, initial results from L-selectin$^{-/-}$ mice support the need for $CD4^+$ T cells, and that such requirement occurs within the LN, as L-selectin is required for trafficking into the LN and loss of L-selectin would prevent entry of $CD4^+$ T cells into the LN (Bradley *et al.*, 1994, Murphy *et al.*, 2008).

In considering studies that suggest mechanisms of vascular growth in the LN that would potentially be applicable to remodeling of LN arteriole, those demonstrating VEGF and DCs as key LN vascular growth regulators stand out (Chyou *et al.*, 2008, Webster *et al.*, 2006, Shrestha *et al.*, 2010), and leads to proposing that DCs and VEGF drive expansion of the LN arteriole. Below is an analysis of how results presented in this study support a role for DCs in $CD4^+$ T cell dependent LN arteriole remodeling.

However, direct evidence of a role for VEGF requires further study and is discussed as a future direction.

DCs within the reactive LN are optimally positioned to act on upstream HEVs and vasculature as they wrap themselves around HEVs to screen lymphocytes entering the LN and have significant interaction with $CD4^+$ T cells (Bajenoff, *et al.*, 2003, Murphy *et al.*, 2008) and may transmit signals to the upstream vasculature. Furthermore, the depletion of DCs results in decreased lymph node hypertrophy and EC proliferation, both of which correspond to the timeline of arteriole remodeling. The degree of EC proliferation within stimulated LN has also been shown to correspond proportionally to the number of DCs in the LN (Webster *et al.*, 2006). This may also explain the relationship of B cells to LN vascular growth as B cells, via VEGF driven lymphangiogenesis, were recently shown to enhance DC migration to the lymph node (Angell *et al.*, 2006, Shrestha *et al.*, 2010); B cells may be facilitating vascular growth via enhancing DC migration, which subsequently drives other forms of vascular growth such as HEVs and feed arteriole expansion. However, studies by collaborators provide evidence against this, as mice lacking B cells had no deficit in LN enlargement and loss of $CD4^+$ T cells resulted in decreased B cell recruitment into the node. One potential explanation for these conflicting reports may be an intermediate step between B cells and DCs. As B cells, and related VEGF expression, have been linked to the expression of LTβR, we propose that LTβ, produced by the FRC as previous demonstrated (Browning *et al.*, 2005, Chyou *et al.*, 2008, Kumar *et al.*, 2010) or alternatively, produced by or controlled by DCs in a $CD4^+$ T cell dependent manner may be such an intermediate. While this hypothesis remains to be investigated, LN enlargement was found to be

dependent upon $CD4^+$ T cell interaction with DCs through MHC II to TCR and through CD40 and CD40L interface. Dr. Iwasaki's groups further showed that this was a critical factor in facilitating naïve polyclonal $CD8^+$ T cells entry into the LN, which resulted in decreased magnitude of CTL response to infectious agent (Kumamoto *et al.*, 2011). Collectively, these results, in combination with our own, identifies $CD4^+$ T cell driven vascular growth, of the LN feed arteriole, through DC interaction, as a mediator of CTL responses to intracellular pathogens. Alternatively, despite strong evidence for DCs in LN vascular growth and the interaction of $CD4^+$ T cells with DCs, which regulates cellular entry into the LN and LN enlargement, another possibility is that antigen-specific $CD4^+$ T cells are also acting independently to induce the recruitment of naive $CD4^+$ T cells and induction of subsequent arteriole remodeling (Kumamoto *et al.*, 2011). This mechanism could be potentially driven by the production of interferon gamma, which has been shown to enhance migration into the LN (Hendriks *et al.*, 1989, Kraal *et al.*, 1994).

The absence of remodeling seen in old mice also supports the importance of $CD4^+$ T cells in arteriole remodeling, as aged mice show decreased $CD4^+$ T cell numbers, decreased proliferation of antigen specific $CD4^+$ T cells, and a marked decline in ability to mount effective adaptive immune responses (Linton *et al.*, 2004). However, further experiments are needed to reveal changes in the aged LN in response to HSV infection to conclude whether low numbers or functionality of $CD4^+$ T cells are responsible for defects in remodeling seen in aged mice as other alternatives are plausible. One such alterative reason for lack of arteriole remodeling may be the result of vascular dysfunction during infection seen with aging indicated by the decrease in arteriole responsiveness to phenylephrine. What was most surprising about this observation was

that the blunted response was only seen at day seven after infection and not at day zero. Had a blunted response been observed in all old mice, regardless of days p.i., this would be indicative of the aging disease process had a pathogenic effect on the feed arteriole. However, as the blunted response is only seen during infection, which is not seen in adult mice, this suggests that the infection is causing pathology within the vessel that changes responsiveness to the action of the α_1-adrenergic receptor agonist on the smooth muscle cells of the arteriole. Why this is seen during infection of old mice and not young remains unclear and has not previously been noted in the literature. However, a greater understanding of vascular dysfunction resulting during infection with aging would provide further insight into decreasing immunity and vascular dysfunction during aging.

Even though findings within this chapter generate a number of new future directions and research questions, the overall goal is fulfilled as the first steps within determining the mechanism of arteriole remodeling were taken. Arteriole remodeling is shown to be a $CD4^+$ T cell dependent process through interaction with DCs within the LN and links to priming of CTL that are vital for pathogen clearance. These findings also agree with previous studies of the integral nature of VEGF and DCs in the LN and highlight the need for continued study of LN arteriole remodeling and speak to the therapeutic potential in learning to manipulate immune response through altering of the LN microvasculature. For example, it could be used to boost immune response, by facilitating faster and/or increased entry into lymph nodes which would serve to decrease the rate limiting process of screening for cognate lymphocytes and priming of CTLs.

CHAPTER FIVE – Vascular Mediators in Lymph Node Arteriole Remodeling

5.1 Introduction

During infection, lymph nodes (LNs) serve as an interface between the innate and adaptive immune system and are the site of induction of antigen specific cytotoxic T lymphocyte (CTL) responses that are critical to fighting intracellular pathogens. In previous chapters, the full spectrum and type of arteriole remodeling throughout the course of infection was elucidated and immune mediators were considered in the remodeling process as the magnitude and kinetics of remodeling mimicked previously noted changes in LN vascularity driven by the immune system (Angell *et al.*, 2006, Chyou *et al.*, 2008, Liao & Ruddle, 2006,Webster *et al.*, 2006). This revealed arteriole remodeling to be dependent upon the presence of $CD4^+$ T cells and driven by $CD4^+$ T cell interaction with DCs which was critical factor in facilitating naïve polyclonal $CD8^+$ T cells entry into the LN, which resulted in decreased magnitude of CTL response to infectious agent (Kumamoto *et al.*, 2011). While this identifies $CD4^+$ T cell driven vascular growth of the LN feed arteriole as a mediator of CTL responses to intracellular pathogens, further study of the vascular changes that occur within the LN arteriole and the mechanism driving its expansion are critical components to understanding the potential therapeutic applications of using the LN arteriole to influence immune response.

Having explored immune mediators, investigation of the other side of this immune-vascular phenomenon, vascular mediators, was the next direction in exploring the mechanism of arteriole remodeling. Original reports of arteriole remodeling during infection showed a blunted degree of arteriole constriction with pharmacological inhibition of NOS three days following infection. This demonstrated a decrease in nitric

oxide mediated vasodilation as NOS is required for NO production, which acts on SMCs through guanylate cyclase to induce vasodilation (Soderberg *et al.*, 2005, Vanhoutte, 2003). Despite this interesting observation, whether this state of decreased response to NOS inhibition mirrors the pattern of arteriole remodeling or is transient on specific days following infection remains to be determined. To address this, arteriole response to L-NAME, which is a global inhibitor of NOS, was considered throughout the course of infection and subsequently revealed that blunted constrictive response to L-NAME is transient.

Blunted response to NOS inhibition also suggests a role for NOS in mediating arteriole remodeling, and notably, NO is important in lymphocyte trafficking, which is a key component in arteriole remodeling (Kumanmoto *et al.*, 2011), with NO noted as inhibitor of leukocyte adhesion to endothelium, and L-NAME treatment resulting in increased adherence and emigration (Akimitsu *et al.*, 1995, Kubes, 1991). NO is also a mediator of ICAM-1 binding by leukocytes and a mediator of altered hemodynamics, which through impact on leukocyte distribution within vessels and activation of selectins, including L-selectin, and adhesion molecules impacts cellular trafficking (Alon & Dustin, 2007, Finger *et al.*, 1996, Kubes *et al.*, 1991, McEver & Zhu, 2007, Ridger *et al.*, 2008, Sucosky *et al.*, 2009). Beyond its impact on immune cells, NO is a known regulator of VEGF induced vascular growth; mice deficient in eNOS do not respond to VEGF and subsequently have defective angiogenesis, arteriogenesis, and mural cell recruitment and increased levels of VEGF are inducible through increased eNOS levels (Benest *et al.*, 2008, Yu *et al.*, 2005). NO is also a regulator of EC proliferation, which is a key component of LN vascular growth mediated through VEGF and DCs (Metaxa *et al.*,

2008, Webster *et al.*, 2006). The later of which was linked to arteriole remodeling given the interaction DC interaction with $CD4^+$ T cells of which arteriole remodeling is dependent (Kumamoto *et al.*, 2011). Therefore, given the role of NO in lymphocyte trafficking and VEGF and the key role of lymphocytes in arteriole remodeling, the hypothesis that eNOS was required for arteriole remodeling and LN hypertrophy was investigated using both pharmacological inhibition (systemic treament with L-NAME) and genetic ablation models ($eNOS^{-/-}$ mice).

In addition to eNOS, a seconded vascular mediator, TNF-alpha was considered. TNF-alpha, like NO, is noted to play a role in leukocyte trafficking. In skeletal muscle, TNF-alpha recruits T_H1 cells (Norman *et al.*, 2008) and in aging models of delayed hypersensitivity, memory $CD4^+$ T cells are prevented from migrating due to a lack of TNF-alpha secretion (Agius *et al.*, 2009). TNF-alpha has been shown to be an inducer of vascular remodeling acting through TNF receptors on vascular ECs during infection, as well as a mediator of angiogenesis *in vivo,* and an inducer of NOS during HSV infection (Baluk *et al.*, 2009, Benecia, *et al.*, 2003, Frater-Schroder *et al.*, 1987, Leibovich *et al.*, 1987). Therefore, with the role of TNF-alpha in facilitating changes in NO levels, vascular remodeling, and dynamics of lymphocyte migration, the hypothesis that TNF-alpha was required for arteriole remodeling became a study focus and investigated using TNF-$alpha^{-/-}$ mice.

Conclusions regarding the role of TNF-alpha in arteriole remodeling led to questions regarding the mechanism by which TNF-alpha acts on the LN and to investigation of the role of mast cells, as mast cells are large producers of TNF-alpha (Murphy *et al.*, 2008). While mast cells have a well established function in innate

immune response, it is only recently that their important role in adaptive immunity has begun to be appreciated based on the collective findings of McLachlan and colleges (2008, 2003). Markedly, the degranluation of mast cells in the footpad (induced either with intradermal bacterial challenge or mast cell activator compound 48/80) has been shown to induce cellular accumulation of naïve T lymphocytes in the draining popliteal lymph node and hypertrophy of the dLN itself. This hypertrophy peaked twenty-four following stimulation and resolved by fourty-eight hours. Increased cellularity and DC numbers characterized hypertrophy, with mast cell deficient mice showing reduced LN hypertrophy. Furthermore, these findings were attributable to the release of presynthesized TNF-alpha that drained into the LN from the footpad, with TNF protein levels increasing in the LN within one hour of stimulation (McLachlan *et al.*, 2008, McLachlan *et al.*, 2003). Such remote control of the LN has been shown in other cases; monocyte recruitment to the LN was upregulated by selective trafficking of MCP-1 for inflamed skin to the HEVs dLN as evidenced by IVM staining (Palframan *et al,* 2001). These findings lead to the hypothesis that activation of mast cells may facilitate remodeling of the dLN feed arteriole in the process of initiating adaptive immunity. Therefore, the role of mast cells was investigated using mast cell deficient mice in combination with gross examination of LN for evidence and hypertrophy and IVM to explore requirement for LN arteriole remodeling.

5.2 Results

Based on the previously established importance of eNOS in regulating cell migration, vascular growth, endothelial cell proliferation, and modulation of VEGF in other contexts (Benest *et al.*, 2008, Chyou *et al.*, 2008, Norman *et al.*, 2008, Yu *et al.*, 2005), the role of eNOS in arteriole remodeling was investigated. Genetic ablation of models lacking expression of eNOS showed an inability to remodel LN arterioles in response to infection (Figure 13A, B). Seven days following infection, the point at which maximal remodeling was seen in wild-type mice (Figure 3), $eNOS^{-/-}$ showed no increase in resting or maximal diameter. However, they still maintained robust response to phenylephrine (Figure 13C).

To confirm ablation results and address any possibility that lack of remodeling was an artifact of genetic manipulation, we looked at LN arteriole remodeling capacity of wild-type mice treated systemically with NOS inhibitor L-NAME (Figure 13D). In accordance with $eNOS^{-/-}$, pharmacological inhibition of NOS resulted in no significant change in arteriole diameter during infection. This clearly demonstrates the requirement for eNOS expression in facilitating LN arteriole remodeling and is underscored when comparing the percent increase in resting and maximal arteriole diameter relative to day zero diameters in WT, $eNOS^{-/-}$, and L-NAME treated mice at day seven p.i., (Figure 13E) which shows significantly blunted response when eNOS is ablated or NOS function is blocked.

Figure 13: eNOS is Required for Lymph Node Arteriole Remodeling During Infection. A. Resting and maximal (+nifedapine) arteriole diameter at days zero and seven p.i. in $eNOS^{-/-}$ mice with $TK^{-}HSV$-2 **B.** Representative images of resting and maximal diameter $eNOS^{-/-}$ arterioles at days zero and seven after infection where arterioles are indicated by green arrows. **C.** Percent vessel constriction with respect to resting vessel diameter of $eNOS^{-/-}$ LN arterioles at day zero and seven p.i. in response to PE applied in fold increases from 10^{-9} to 10^{-5}M. **D.** Resting and maximal (+SNP) arteriole diameter at days zero and seven p.i. with $Tk^{-}HSV$-2 in mice treated systemically with L-NAME. **E.** Resting and maximal vessel diameters (% of uninfected) of WT, $eNOS^{-/-}$ and L-NAME treated mice. For $eNOS^{-/-}$ n=4 and 5 respectively for days zero and seven vessel diameters, and n=4 for all PE data points. For L-NAME treatment, n=4 for all data points. For WT n=5 at day seven p.i.. In all cases, one arteriole was studied per animal. *$p<0.05$, **$p<0.01$, and ***$p<0.001$.

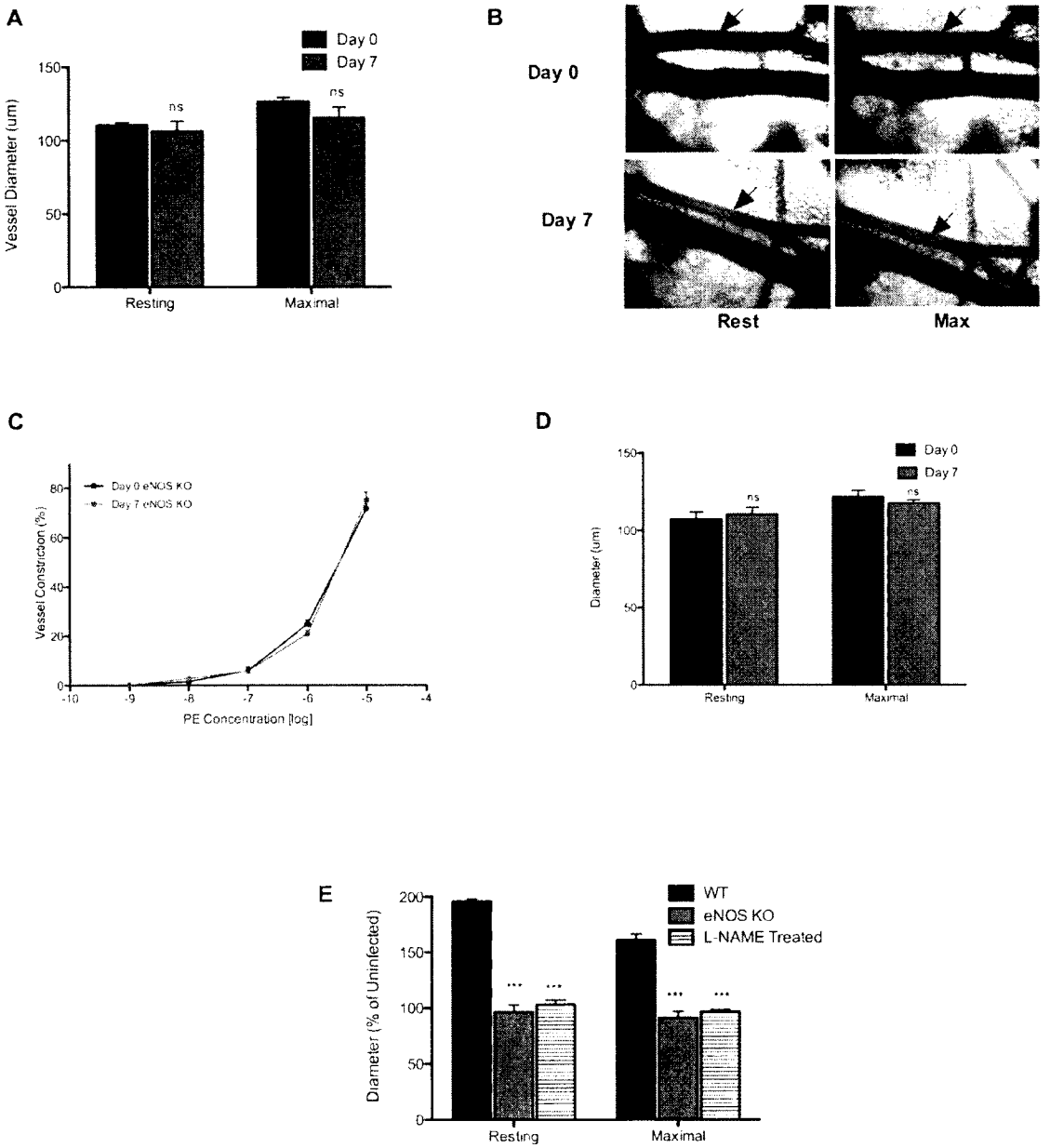
A
Day 0
Day 7
Vessel Diameter (um)
150
100
50
0
ns
ns
Resting
Maximal
B
Day 0
Day 7
Rest
Max
C
Day 0 eNOS KO
Day 7 eNOS KO
Vessel Constriction (%)
80
60
40
20
0
-10
-9
-8
-7
-6
-5
-4
PE Concentration [log]
D
Day 0
Day 7
Diameter (um)
150
100
50
0
ns
ns
Resting
Maximal
E
WT
eNOS KO
L-NAME Treated
Diameter (% of Uninfected)
200
150
100
50
0
***
***
***
***
Resting
Maximal

The absence of such arteriole remodeling as a result of $CD4^+$ T cell deficiency was shown to result in decreased LN hypertrophy due to decreased cellular trafficking (Kumamoto *et al.*, 2011). To examine whether eNOS deficiency had the same result, lymph node size and weight following infection was examined. This investigation reavealed that LNs from $eNOS^{-/-}$ showed no increase in size throughout the course of infection (Figure 14A). Furthermore, weight of isolated $eNOS^{-/-}$ lymph nodes were similar at days zero and seven following infection (Figure 14B), and demonstrates that eNOS is required for LN arteriole remodeling and subsequently lymph node hypertrophy.

Figure 14: eNOS is Required for Lymph Node Hypertrophy. A. Representative images of isolated eNOS$^{-/-}$ lymph nodes at days zero, one, five, and seven p.i.. **B.** Lymph node weights of isolated eNOS$^{-/-}$ lymph nodes following infection at days zero and seven p.i..

A

Day 0 1 5 7

B

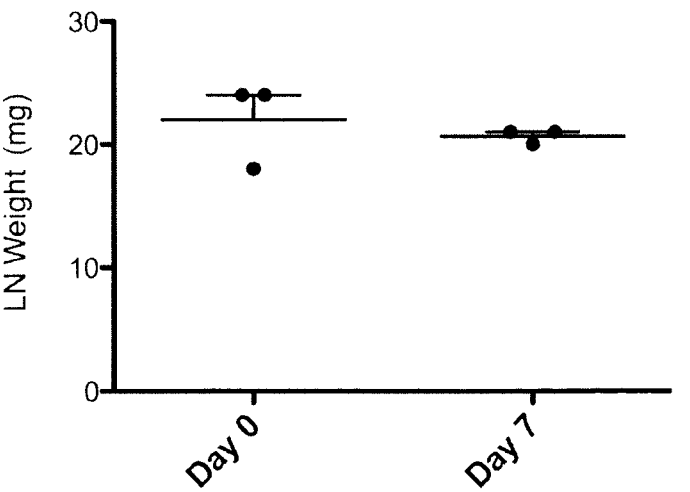

Given the importance of eNOS for remodeling, initial reports that described blunted response to inhibition to NOS at day three p.i. was considered (Soderberg *et al.*, 2005) as it remained unknown if this blunted response continued throughout the course of infection similar to remodeling of the arteriole. This was addressed by looking at vessel response to L-NAME perfusion over the intravital microscopy preparation of the feed arteriole of C57 BL/6 mice at days zero, one, three, five, seven, nine, and thirty-five p.i. (Figure 15A, B). Similar to previous findings, the arteriole showed blunted constriction to L-NAME three days p.i., however, this blunted response was not noted at day one p.i., but did persist through day five p.i. (Figure 15A). Notably, by day 7 p.i. response had returned to values similar seen at day zero p.i. and remained there through days nine and thirty-five p.i. (Figure 15B), and demonstrates a pattern of transient decrease in NOS activity during infection.

As arteriole remodeling was dependent on $CD4^+$ T cells, the question of whether the same mechanism was regulating NOS activity in the arteriole arose. To address this, the effect on L-NAME treatment on vessel diameter was studied in $CD4^{-/-}$ mice at days zero, three, and seven p.i. (Figure 15C) and showed that in the absence of $CD4^+$ T cells, the arteriole still shows a blunted response to NOS inhibition at day three p.i., which returns to baseline levels by seven days p.i.. Collectively, these results demonstrate that the transient decrease in NOS activity seen in WT mice (Figure 15A, B) is not dependent upon $CD4^+$ T cells.

Figure 15: Nitric Oxide Levels are Variable During Infection and CD4 Independent. Percentage of vessel constriction in response to perfusion of 100μM L-NAME solution over the vessel preparation **A**. Days zero, one, three, and five p.i. in C57 BL/6 mice. **B**. Days zero, seven, nine, and thirty-five p.i. in C57 BL/6 mice **C**. zero, three, and seven days p.i. in $CD4^{-/-}$ mice. Data represents percent vessel constriction in diameter ± SEM where one arteriole was studied per animal. *$p<0.05$ **$p<0.01$, and ***$p<0.001$.

A

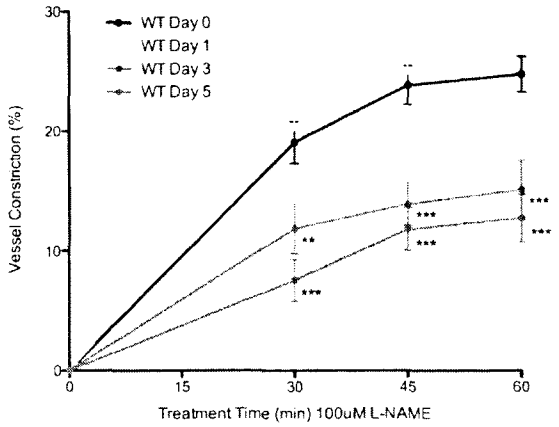
WT Day 0
WT Day 1
WT Day 3
WT Day 5
Vessel Constriction (%)
Treatment Time (min) 100uM L-NAME

B

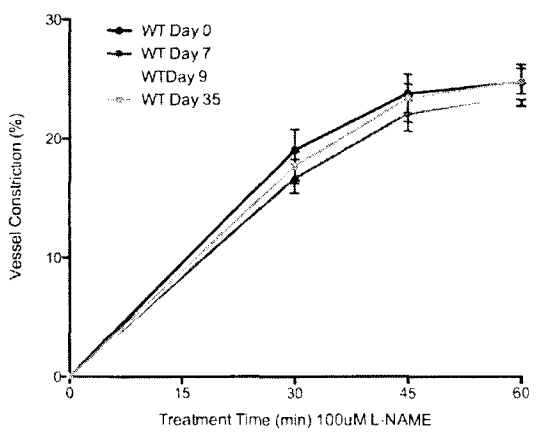
WT Day 0
WT Day 7
WTDay 9
WT Day 35
Vessel Constriction (%)
Treatment Time (min) 100uM L-NAME

C

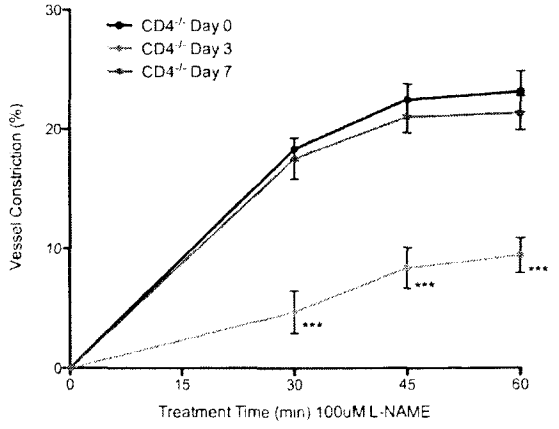
CD4-/- Day 0
CD4-/- Day 3
CD4-/- Day 7
Vessel Constriction (%)
Treatment Time (min) 100uM L-NAME

Next, based on studies previous studies demonstrating TNF-alpha as a key regulator of LN hypertrophy and as mediator of vascular changes (Baluk *et al.*, 2009, McLachlan *et al.*, 2008, McLachlan *et al.*, 2003), the ability of the LN feed arteriole to remodel in the absence of TNF-alpha was examined. Three and seven days p.i., mice deficient in TNF-alpha showed no increase in resting or maximal vessel size compared to day zero p.i. (Figure 16A, B), but still showed excellent response to PE that was comparable to wild-type day zero controls (Figure 17A). Additionally, H&E stained vessels showed no change in vessel morphology (Figure 17B). Furthermore, loss of TNF-alpha did not change vessel response to L-NAME at days three and seven during infection; arteriole response to application of L-NAME at day zero in Tnf-alpha deficient mice was similar to wild-type mice, and a significant decrease in response is seen at day three p.i., which returns to normal levels by day seven p.i. (Figure 17C). Collectively, this data demonstrates that TNF-alpha is required for LN arteriole remodeling during infection, but does not mediate the transient drop in vessel response to NOS inhibition.

Figure 16: Role of TNF-alpha in Lymph Node Arteriole Diameter. A. Resting and maximal (+100μM SNP) arteriole diameter zero, three, and seven days after i.vag. infection in TNF$\alpha^{-/-}$ mice with n= 5 for day zero and n=4 for days three and seven respectively. **B**. Representative image of resting arterioles with arterioles indicated by green arrows. Data represents mean diameter ± SEM (A), where one arteriole was studied per animal. *$p<0.05$, **$p<0.01$, ***$p<0.001$, ns= not significant.

A

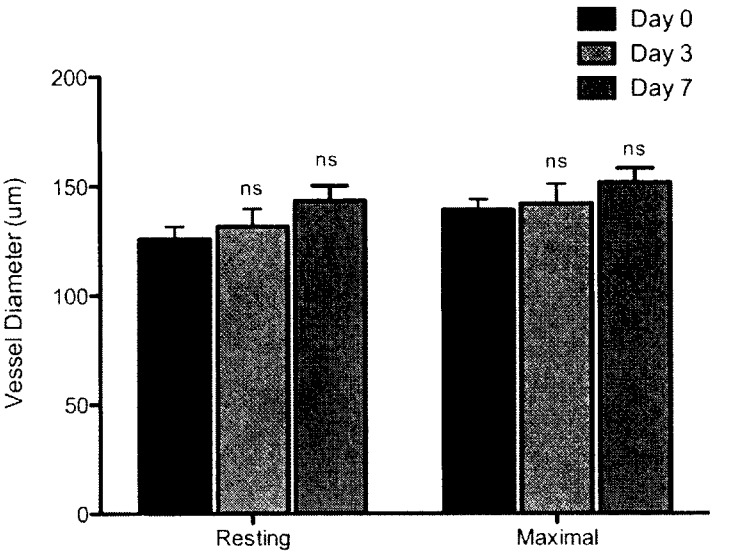
Day 0
Day 3
Day 7
200
150
100
50
0
Vessel Diameter (um)
ns
ns
ns
ns
Resting
Maximal

B

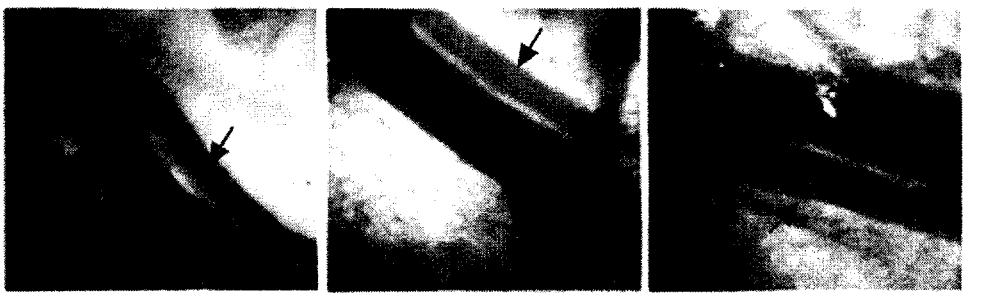
Day 0
Day 3
Day 7

Figure 17: Role of TNF-alpha in Lymph Node Arteriole Vasoactive Profile During Infection. A. Phenylephrine (PE) dose response (percent vessel constriction) from 10^{-9}M to 10^{-5}M at zero (n=5), three (n=4), and seven (n=4) days p.i. in TNF$\alpha^{-/-}$ mice in comparison to WT C57 BL/6 mice (n=5) **B.** Representative images of H&E stained arteriole cross-sections in TNF$\alpha^{-/-}$ mice zero and seven days p.i.. **C**. Percentage of vessel constriction in TNF$\alpha^{-/-}$ mice in response to perfusion of 100μM L-NAME at days zero (n=5), three (n=4), and seven (n=4) following infection. Data represents mean vessel constriction (A, C) ± SEM where one arteriole was studied per animal. *$p<0.05$, **$p<0.01$, and ***$p<0.001$.

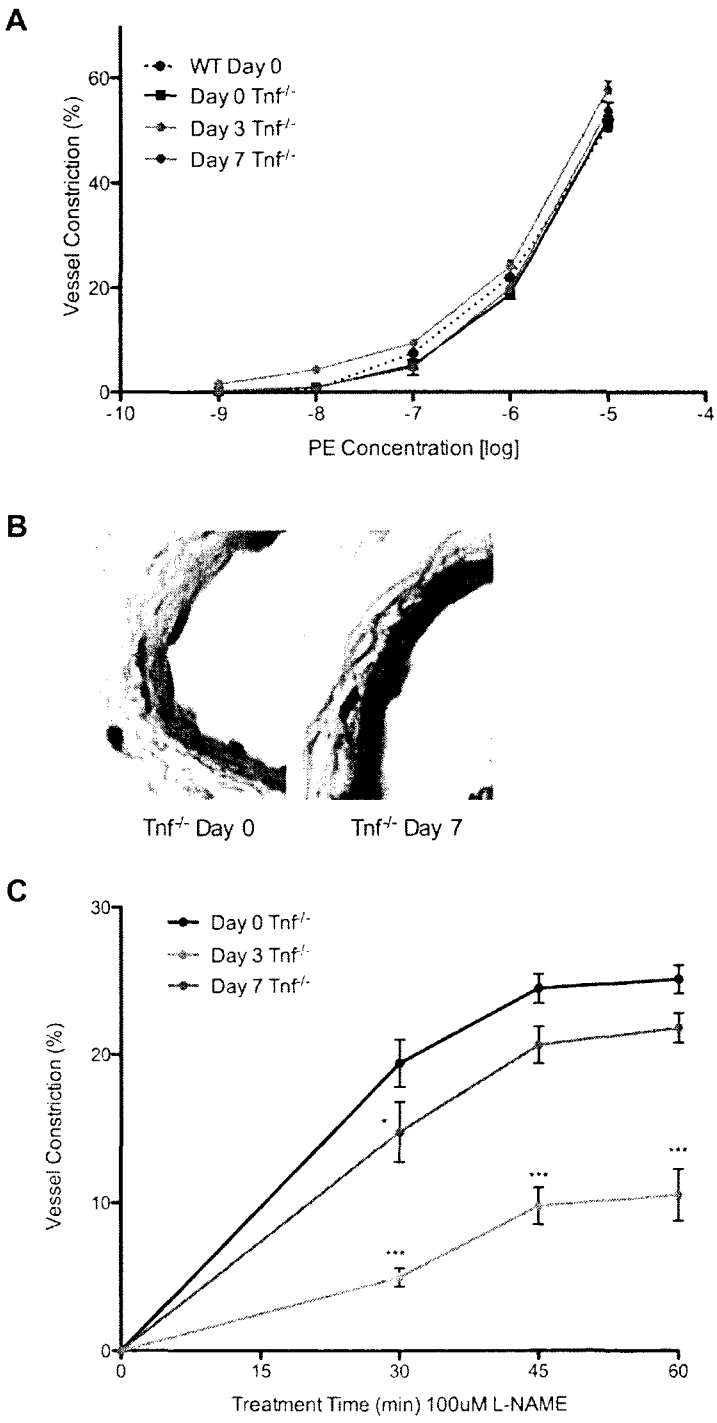
A
WT Day 0
Day 0 Tnf-/-
Day 3 Tnf-/-
Day 7 Tnf-/-
Vessel Constriction (%)
PE Concentration [log]
B
Tnf-/- Day 0
Tnf-/- Day 7
C
Day 0 Tnf-/-
Day 3 Tnf-/-
Day 7 Tnf-/-
Vessel Constriction (%)
Treatment Time (min) 100uM L-NAME

Reports that cited TNF-alpha as a mediator of LN expansion provided evidence that the key source of TNF-alpha was mast cells; significant levels of mast cell degranulation is noted within two hours of challenge and mice given TNF-alpha-deficient mast cells have blunted LN hypertrophy (McLachlan *et al.*, 2008, McLachlan *et al.*, 2003). This, in combination with the requirement for TNF-alpha demonstrated above, prompted investigation of the requirement for mast cells in arteriole remodeling. Mice deficient in mast cells showed significant remodeling seven days p.i., in comparison to day zero controls (Figure 18A). However, vessels were still significantly smaller than day seven wild-type mice (Figure 18B). Furthermore, mast cell deficient mice demonstrated a moderate level of LN hypertrophy (Figure 18C). Collectively, this suggests that arteriole remodeling is partially dependent upon mast cells and that mast cells contribute to the magnitude of arteriole remodeling.

Figure 18: Role of Mast Cell in Lymph Node Arteriole Remodeling. A. Resting and maximal (+30μM Nifedapine) arteriole diameter at zero (n=4) and seven (n=5) days after i.vag. infection in mast cell deficient mice **B**. Comparison of maximal arteriole diameter in wild-type (C57 BL/6) (n=5) and mast cell deficient mice (n=5) at day seven following infection **C**. Representative images of lymph nodes from mast cell deficient mice at days zero and seven following infection. Data represents mean vessel diameter (A, B) ± SEM where one arteriole was studied per animal. *$p<0.05$, **$p<0.01$, and ***$p<0.001$.

A

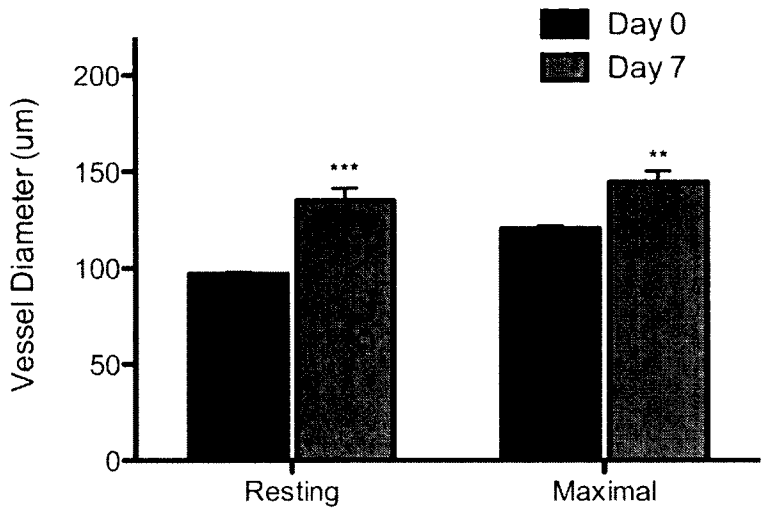
Day 0
Day 7
Vessel Diameter (um)
200
150
100
50
0
***
**
Resting
Maximal

B

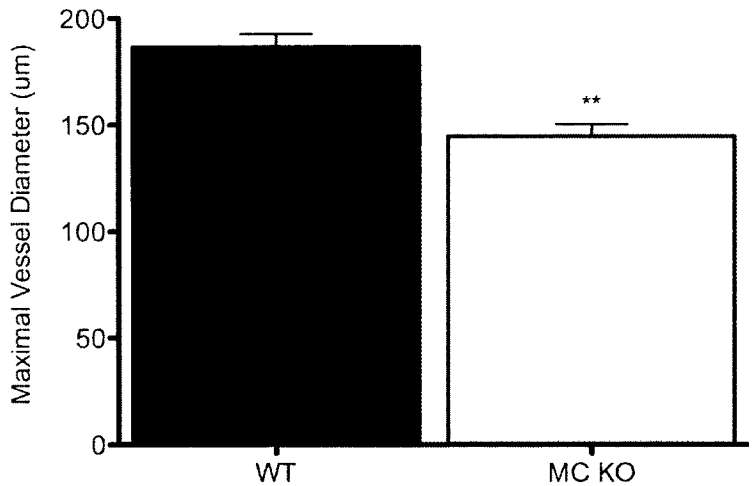
Maximal Vessel Diameter (um)
200
150
100
50
0
**
WT
MC KO

C

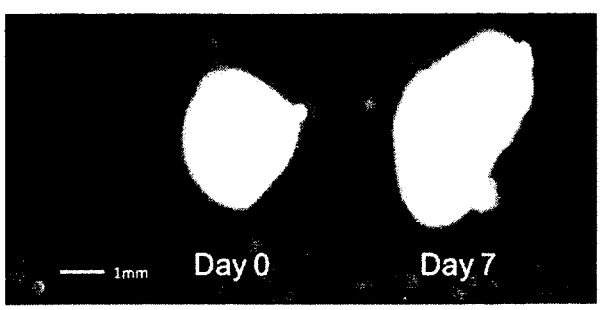
1mm
Day 0
Day 7

5.3 Discussion

Presented here are the first studies to implicate NO in the regulation of lymph node expansion, as the role of NO in the vasculature of the LN and its subsequent impact on immune response has never been studied outside of our initial report (Soderberg *et al.*, 2005). Results, using both genetic and pharmacological means, show that the mechanism of arteriole remodeling is eNOS dependent and that constriction as a result of L-NAME perfusion over the arteriole is decreased three and five days p.i.. Blunted response to NOS inhibition three and five days p.i., implies a change in NOS activity and subsequently NO production on these days. Alternatively, it could imply a change in NO bioavailability and NO acting upon the vessel and influencing diameter. Interestingly, this process was not dependent on $CD4^+$ T cells as arteriole remodeling was noted to be. Together, these data suggest that during infection the LN feed arteriole has decreased NOS activity contributing to vessel dilation three and five days p.i. and that this reduction, unlike the mechanism of remodeling, is not dependent upon $CD4^+$ T cells. This, in turn, leads to the conclusion that the mechanism governing NOS activity within the LN feed arteriole during infection is different than that regulating vessel remodeling and leaves the mechanism of blunted response to NOS inhibition as a future direction.

While the mechanism of the blunted response to NOS inhibition remains to be elucidated, so does its function. One hypothesis about potential function is to facilitate migration into the lymph node, which is supported by the lack of hypertrophy seen in $eNOS^{-/-}$ LNs following infection. Additionally, previous studies have shown NO to inhibit T cell rolling along the endothelium, with inhibition of NOS leading to increased rolling, adhesion, and emigration (Akimitsu *et al.*, 1995, Kubes *et al.*, 1991, Sundrani *et*

al., 2000), therefore, the arteriole may facilitate T cell rolling by down-regulating NO production. However, complete shut-down of NO would be detrimental, as evidenced by the lack of LN hypertrophy in $eNOS^{-/-}$ mice and with pharmacological inhibition of NOS with L-NAME treatment. Lack of eNOS may be inhibitory to LN arteriole remodeling due to its impact on VEGF, which is key in LN vascular growth and EC proliferation (Webster *et al.*, 2006). eNOS has been shown previously to be required for a response to VEGF outside the LN. In ischemic conditions, loss of eNOS results in reduction in angiogenesis, arteriogenesis and mural cell recruitment (Murohara *et al.*, 1998, Yu *et al.*, 2005) and exogenous delivery of eNOS has been shown to increase VEGF expression and give rise to mature phenotype of newly formed arterioles and capillaries (Benest *et al.*, 2008). Alternatively, change in shear stress triggering EC proliferation in response to high flow, which would be required for increased delivery of blood to the LN and outward eutrophic remodeling, may also be a mechanism behind the requirement of eNOS dependency in the LN (Metaxa *et al.*, 2008).

It is also arguable that the blunted response to L-NAME, suggesting decreased NO, is contradictory to increases in VEGF that was previously proposed to be an player in arteriole remodeling and is key in LN ECs proliferation during infection (Webster *et al.*, 2006). This is because VEGF is known to activate eNOS. Following stimulation of VEGF receptors, increased eNOS expression results from activation of the PI3K/Akt pathways leading to release of eNOS from caveolin-1, which binds eNOS and decreases its activity, with subsequent increased eNOS activity due to phosporylation (Fontana *et al.*, 2002, Papapetropoulos *et al.*, 1997). This means that decreased eNOS would be associated with decreased VEGF, both of which are contradictory to vascular growth.

However, a theory of two separate pathways may harmonize these opposing points. The first pathway being that VEGF levels are unregulated in LN to facilitate vascular growth and that VEGF is secreted and/or signaling is directed upstream to the HEVs and subsequently the arteriole. The second pathway, that decreased NO induced vasodilation at days three and five p.i. are specific to the arteriole and are not affect by VEGF levels in the LN, but may play a role in supporting VEGF secretion by increasing lymphocyte trafficking. This is further supported by findings that while $CD4^+$ T cells and TNF-alpha were both required for LN arteriole remodeling, but the observed transient decrease in NO was not.

The second part of investigation of vascular mediators of LN arteriole expansion focused on TNF-alpha, and demonstrated the process to be TNF-alpha dependent. TNF-alpha is a known regulator of vascular remodeling, EC proliferation, and T cell migration but is known to act early in the process of vascular remodeling. This suggests that TNF-alpha may act early in the LN arteriole remodeling process to induce initial stages of EC proliferation and T cell migration. Notably, in the case of M. *pulmonis* infection, increase in TNF-alpha preceded vascular remodeling events and blockade of TNF-alpha resulted in decreased VEGF levels, and leukocyte trafficking and slowed the process of remodeling of blood vessels (Baluk *et al.*, 2009), suggesting that TNF in the LN may be required for increased VEGF. TNF-alpha may also be facilitating VEGF expression and subsequent vascular expansion by facilitating DC migration into the LN (Baluk *et al.*, 2009, Frater-Schroder *et al.*, 1987, Leibovich *et al.*, 1987). Later in the arteriole remodeling and infectious process, TNF-alpha may also be acting to limit the magnitude of the inflammatory response within the LN. TNF-alpha been shown to up regulate the

A_{2B} receptor, a receptor for CD73-generated adenosine known to be expressed on HEVs, and the absence of CD73 results in increased trafficking into the LN and vascular permeability, which is abrogated by pharmacological blockade of the A_{2B} receptor. These findings suggest that CD73-generated adenosine may act to limit inflammatory associated permeability within the LN, facilitated by TNF-alpha regulation of the A_{2B} receptor (Tackedachi *et al.*, 2008).

Studies on the requirement of mast cells for arteriole remodeling showed a partial requirement for mast cells; mice deficient in mast cells showed a decreased magnitude of remodeling. Previously, McLachlan and colleges (2003, 2008), showed that TNF-alpha released from mast cells was transmitted upstream to the LN and facilitated LN hypertrophy, including DC and lymphocyte accumulation. This would suggest that if arteriole remodeling was observed to be dependent on lymphocyte accumulation and interaction with DCs and TNF-alpha, it should also be dependent on mast cells. However, this cellular accumulation was transient, in studies by McLachlan and colleges cellular accumulation happened early, spiking at twenty-four hours and declining by fourty-eight hours, indicating requirement for TNF-alpha derived from mast cells acts early in the remodeling process, and that TNF-alpha derived from an alternative sources may act throughout the remainder of the remodeling process, although mast cell derived TNF-alpha may facilitate increased magnitude of response, subsequently suggesting that this may be used in the future to increase the magnitude of arteriole remodeling and, therefore, the rate of screening for cognate lymphocytes.

CHAPTER SIX – CONCLUDING REMARKS

6.1 Conclusions

Historically, microcirculation and immunity appear to be mutually exclusive physiological components. However, beyond it's traditional role of nutrient, oxygen, and waste exchange, the microcirculation plays a varied and key role in immune functions. These functions range from the circulation and trafficking of immune cells specific to both inflammation and innate and adaptive immune response to invading pathogens, to expression of immune modulating cytokine and chemokines, and supply of metabolites. Therefore, the evaluation of the interface of microcirculation and immune function represents an interdisciplinary approach to gain new perspectives and insight into vascular physiology, immune function, and therapeutic avenues capable of influencing immune response and combating infection. Lymph nodes present themselves as a particularly noteworthy site to study microvascular-immune interface because they are highly vascularized and are the site of induction of adaptive immune response required for antigen specific responses to infiltrating pathogens (Murphy *et al.*, 2008).

In the LN, adaptive immune response generated through antigen presentation of DCs in search of cognate naïve lymphocytes in order to induce clonal expansion and proliferation giving rise of effector responses. During this induction of adaptive response, hypertrophy and increased cellularity are notable and resolve following on-set of immune response (Soderberg *et al.*, 2005, Murphy *et al.*, 2008). Colligation of studies regarding LN vascularity reveal a large number of studies dealing with HEVs and older studies on general increases in blood flow to the LN during immune response. It also becomes apparent that there is relatively little known about the upstream regulation of blood flow

to the LN within the vasculature. In fact, the only study to do so first identified the phenomenon of remodeling of the LN arteriole and demonstrated its importance in facilitating delivery of naïve lymphocytes into the LN and increasing the screening rate for antigen specific T cells. As this is the rate-limiting step in induction of adaptive immune response, arteriole remodeling was singled out as a novel factor in immune regulation (Soderberg *et al.*, 2005). Therefore, in order to understand the phenomenon of LN arteriole remodeling during infection and begin to appreciate its significance, the following objectives were set forth:

(i) To elucidate the extent and nature of vascular remodeling within draining lymph nodes during infection upstream of HEVs at the arteriolar level and consider the potential impact of such remodeling on health and disease.

(ii) Begin to elucidate the mechanism of draining lymph node vascular remodeling in order to identify future targets for control of LN vascular supply.

The data provided in the preceding chapters successfully fulfills these objectives by providing the complete timeline and magnitude of arteriole remodeling, demonstrating the outward eutrophic nature of the remodeling and identifying $CD4^+$ T cells, TNF-alpha, eNOS, and mast cells as key players. Below, findings of this study are highlighted and a working hypothesis on the mechanism of remodeling is suggested. Furthermore, future directions that will help to refine and add to this working model are proposed.

Timeline and Magnitude of Arteriole Remodeling

The first course of action in further investigating arteriole remodeling was to determine the kinetics and magnitude of remodeling throughout infection. This revealed that arteriole diameter becomes significantly larger, in both the resting and maximal diameters states, as early as one day following infection. Subsequently, diameters continue to increase until a peak is reached seven days following infection. By day nine, arteriole diameter has already begun to significantly decrease from the noted peak, and diameters return to baseline by five weeks following infection (Figure 19).

In correlating this to the timeline of infection, a rapid increase occurs during the first day following infection during innate responses is seen. Subsequently, arteriole diameter continues to increase steadily until day seven in correlation with the cellular accumulation with the dLN (Soderberg *et al.*, 2005). Following induction of adaptive response, CTLs begin migrating to the vaginal mucosal infection site between day three and five following HSV-2 infection (Nakinishi *et al.*, 2009), arteriole diameter begins to fall and continues to decrease corresponding to the clearance of infection. This also supports the hypothesis of Hobbs and Hay of hyperemia in the first twenty-four hours followed by vascular growth as we see a rapid increase from day zero to one p.i. and continued increase from day one through seven p.i., but at a more modest rate. Furthermore, hyperemia would involve vasodilation, a point which is supported by that fact that if you integrate the areas under the cure of both the maximal and resting vessel diameters (Figure 19) or compare the percentage increase in comparison to day zero, there a larger change in resting vessel diameter than maximal diameter. Additionally, correlation of LN arteriole remodeling is not exclusive to the dynamics of the immune

system. It also generally correlates to changes in vasculature within the LN including HEV diameter and number, EC proliferation, and changes in blood flow (Hay & Hobbs, 1977, Mebius *et al.*, 1990, Myking, 1980, Soderberg *et al.*, 2005, Webster *et al.*, 2006).

Figure 19: Time-course and Magnitude of Arteriole Remodeling Correlation to the Course of Infection. Following initial viral infection (day zero) a sharp increase in resting and maximal LN arterioles diameters is observed during the initial steps of adaptive immunity on the way to induction of adaptive response. Over the course of the next six days arteriole diameter continues to increase during the adaptive response induction and spikes at day seven. Following the induction of adaptive response and subsequent clearance of infection, arteriole diameters return to baseline.

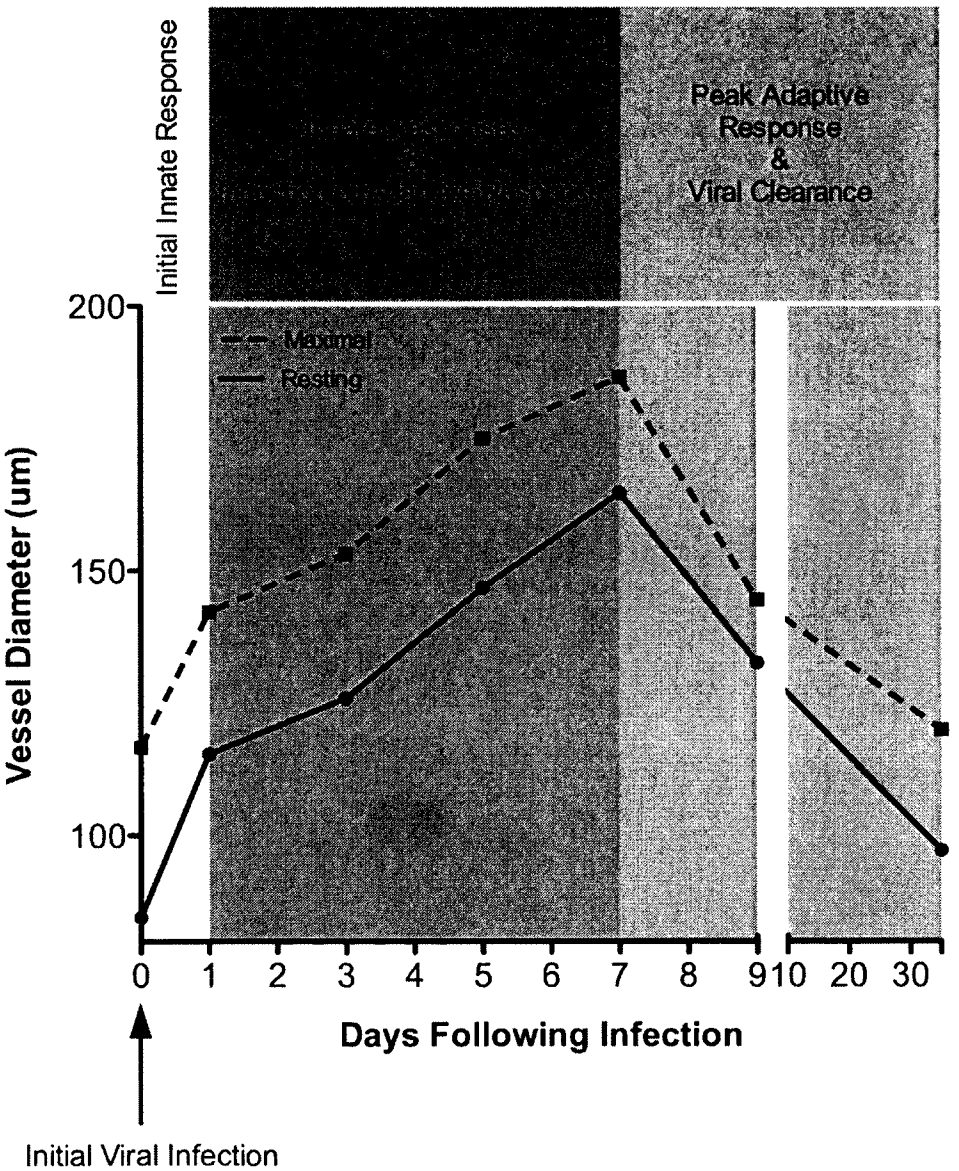
Initial Innate Response
Peak Adaptive Response & Viral Clearance
Maximal
Resting
Vessel Diameter (um)
200
150
100
0 1 2 3 4 5 6 7 8 9 10 20 30
Days Following Infection
Initial Viral Infection

Mechanism of Remodeling

Throughout the preceding chapters we have identified $CD4^+$ T cells, TNF-alpha, eNOS, and mast cells as key players in LN arteriole remodeling during infection. Based on collaborative work, we also implicate this phenomenon in CTL priming through $CD4^+$ T cell interaction with DCs (Kumamoto *et al.*, 2011). When correlating these findings with other studies of vascular growth within the LN, changes in HEVs, and the documented role of vascular mediators in vascular growth, we proposed a number of theories on the various parts of the mechanism governing arteriole remodeling. Figure 20 below summarizes these hypotheses to give an overall depiction of a proposed mechanism of LN arteriole remodeling.

First, during the initial stage of remodeling nitric oxide and TNF-alpha facilitate an initial stage of hyperemia and induce the beginning stages of endothelial cell proliferation. TNF-alpha, predominantly derived from mast cells, also serves to promote lymphocyte and dendritic cell migration into the lymph node. Once in the lymph node DC mediate an increase in VEGF that acts to induce further EC proliferation and vascular growth in a $CD4^+$ T cell dependent manner. Further into the course of infection, decreased NO levels and an ever expanding arteriole facilitate increased $CD4^+$ T cell migration. Additionally, arteriole expansion and $CD4^+$ T cells facilitate B cell migration into the lymph node, which may also contribute to VEGF production and subsequent vascular growth (Figure 20).

Figure 20: Proposed Mechanism of Arteriole Remodeling.

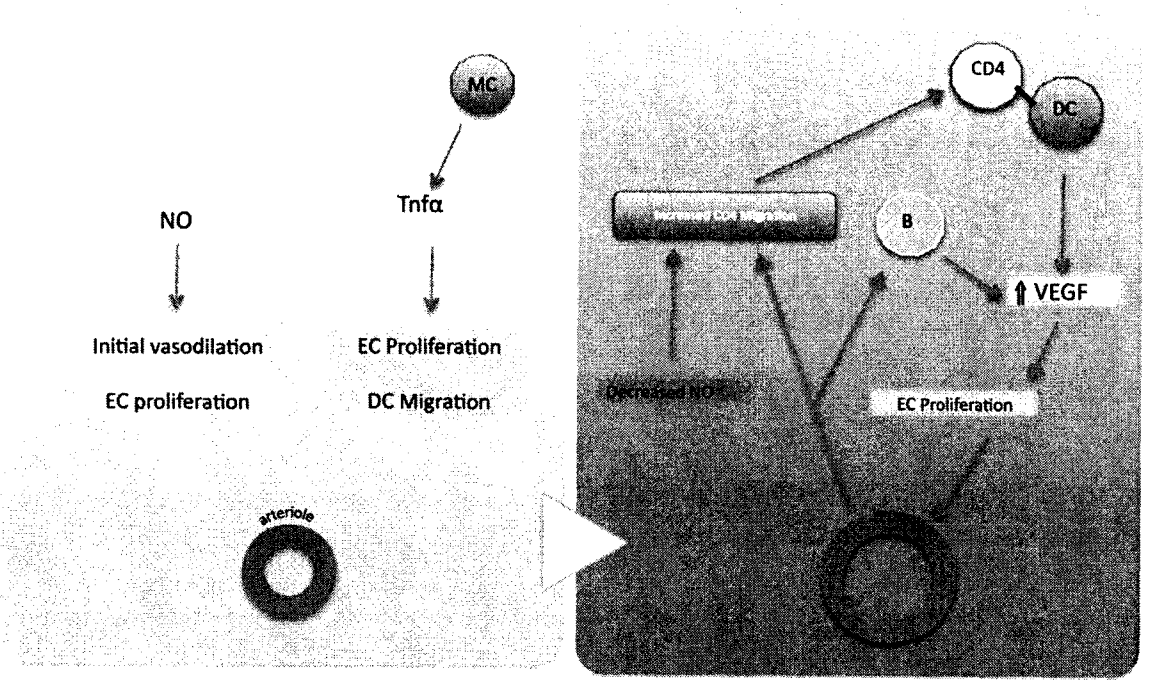
MC
Tnfα
NO
Initial vasodilation
EC proliferation
EC Proliferation
DC Migration
arteriole
CD4
DC
B
VEGF
EC Proliferation

6.2 Future Directions

While the figures above (Figure 19 and 20) provide a summary of the study findings and propose a mechanism of arteriole remodeling, and in doing so fulfill the proposed goals of the project, completion of number of future directions would be helpful confirming or ruling out some of the proposed parts of the mechanism. First, to address EC proliferation within the LN arteriole, experiments staining for BrdU incorporation into the arteriole as an indicator of cell division within the vessel as multiple time-points p.i. are planned. Furthermore, evaluation of hyperemia and changes in vascular leakage that may result between endothelial cells proliferation during infection will be investigated via IVM mediated quantification of leakage of injected 1% FITC-dextran solution. However, while FITC-dextran perfusion occurs through the lymph node arteriole following inter-cardiac perfusion, the large fat pad surrounding the LN is auto-fluorescent (Figure 21). This means that studies using the proposed dye leakage technique would subsequently require either complete removal of the fat or use of a different lymph node that is not obscured by adipocytes.

Once the question of EC proliferation is addressed, understanding reversion to pre-infection size becomes the next step in investigating arteriole remodeling further. Interestingly, of all the studies considered above that noted endothelial cell proliferation within the lymph node, with return to baseline levels, none proposed a mechanism of reversion. If LN arteriole remodeling does in fact require EC proliferation, a proposed mechanism of return to baseline is through rapid apoptosis, which could be easily be explored through a TUNEL assay or screening for biomarkers of apoptosis.

Notably other factors than the mechanism of means by which arteriole remodeling is achieved and resolved should be addressed in order to understand the full vascular profile of lymph node arteriole remodeling. For example, while vessel size increases, do other aspects change within the vessel? Characteristics that should be considered due to their effect on flow within the vessel, and therefore supply to the LN, include blood pressure flow rate, and blood viscosity as this would affect shear stress within the vessel and would add to understanding the possible mechanism acting on the vessel itself or the potential impact of arteriole remodeling or HEV expression of adhesion molecules. The vascular profile would also be more comprehensive with a more complete of understanding of where and when LN arteriole remodeling can be observed and could be addressed looking at alternative pathogens, diseases and sites. In fact, preliminary observations made in the lab indicate that arteriole expansion is observed with vesicular stomatitis virus (VSV), and the use of alternative IVM preparations, such as those for the popliteal and cranial LNs, in order to investigate the arteriole remodeling in alternate sites is a viable option.

Finally, future directions should come to focus on the mechanism driving arteriole remodeling. Based on studies of generalized LN vascular growth that implicated VEGF, a future hypothesis to be explored is that VEGF is the key factor in mediating rapid and robust vascular growth of the LN arteriole and that $CD4^+$ T cells are required for VEGF driven vascular growth. In support of this hypothesis, the timeline of arteriole remodeling corresponds to VEGF levels within stimulated lymph nodes; VEGF levels increase significantly by day one after infection and increase continuously until at least day five following OVA/CFA treatment or transfer of stimulated DCs and correspond to DC

numbers within the LN (Webster *et al.*, 2006). However, further study is required to test this hypothesis and would involve studies confirming the requirement of VEGF for LN arteriole remodeling, although a number of studies clearly supporting a role of VEGF in LN vascular growth (Chyou *et al.*, 2008, Webster *et al.*, 2006, Shrestha *et al.*, 2010). One notable approach to exploring the requirement for VEGF could utilize mice treated with anti-VEGF antibody, as this was a successful approach to confirming the role of VEGF in ECs proliferation in reactive LNs (Webster *et al.*, 2006).

The role of $CD4^+$ tells would also benefit from future experiments, particularly in the context of aged mice as studies of LN T cell numbers and the ability to reconstitute the capacity of the LN arteriole to remodel have yet to be completed. This could be accomplished using FACS analysis of LNs from aged mice as well as reconstitution experiments in which $CD4^+$ T cells from adult mice will be transferred into an aged system. Alternatively, comparison of $CD4^{-/-}$ mice given adult or old $CD4^+$ T cells may be a better option as it would eliminate the other factors within the aged mice that may be effecting remodeling and allow a clearer conclusion regarding whether low $CD4^+$ T cell levels are what is causing a the absence of arteriole remodeling during infection. If such experiments showed a marked decrease in $CD4^+$ T cells in the draining LN and the reinstatement of the ability to remodel, this would suggests that if it were possible to induce arteriole remodeling in an aged model, the quality of immune response during infection would improve given the link between LN enlargement and vascular expansion and CTL responses (Kumamoto *et al.*, 2011).

Finally, the role of NOS is an important future consideration. In order to delineate whether VEGF and eNOS expression is similar in the LN and the arteriole,

immunohistochemistry of arterioles and LNs fixed and isolated at multiple time points p.i. with Tk$^-$HSV-2 in both wild-type (C57 BL/6) and mice genetically deficient in eNOS would be effective. Furthermore, based on previous studies showing that both high levels and ablation of NO expression in blood vessels inhibits CD4$^+$ T cell rolling and subsequent migration, in conjuction with the blunted levels of NO observed in the LN arteriole three and five days p.i., and decreased LN hypertrophy in eNOS deficient mice, suggests that ablation of eNOS decreases cell trafficking into the LN, thereby leading to deficient numbers of CD4$^+$ T cells in the dLN and inhibition of arteriole remodeling (Kubes, 1991, Martinelli *et al.*, 2009). Additionally, decrease of NO levels three and five days p.i., may function to lower NO production to optimal levels for CD4 cell trafficking into the LN. Therefore, to investigate the rate of trafficking of CD4$^+$ T cells into the dLN in both eNOS$^{-/-}$ and C57 BL/6 mice throughout the course of infection with specific attention to changes in trafficking rate between three and five days p.i., cell trafficking could be determined through FACS analysis of cell populations in harvested inguinal lymph nodes in WT and eNOS$^{-/-}$ mice. To address the possibility that CD4$^+$ T cells in eNOS$^{-/-}$ may potentially be intrinsically defective in homing capability, naïve WT CD4$^+$ T cells (isolated using magnetic separation) could be labeled with CSFE and transferred i.v. into eNOS$^{-/-}$ mice prior to infection with subsequent FACS analysis to evaluate accumulation in the LN (Soderberg *et al.*, 2005).

Notably, future experiments designed to determine the mechanism of blunted response to NOS inhibition are more difficult as none of the investigated components that drive arteriole expansion regulate this transient decrease in response. However, one hypothesis that was explored was that the decrease in NO was mediated through

decreased NOS activity, potentially through the binding by caveolin-1. Unfortunately, caveolin-1 deficient mice were found to be highly sensitive to anesthetic protocol utilized and have unstable vascular diameters during IVM thereby indicating that this hypothesis will have to be explored by alternative means in the future.

Despite this difficulty, the above considered future directions form a solid basis from which multiple, original projects can stem. Generally, these projects, would best be focused on further characterizing the nature of LN arteriole remodeling including considering EC proliferation and return of the arteriole to baseline, further elucidating the mechanism driving arteriole remodeling and the subsequent impact on immune response, and exploring the mechanism governing transient NO levels during infection. The diversity and potential impact of these future directions are notable and are based on the findings presented in this study, which was the first to consider LN arteriole remodeling in-depth. Such consideration resulted in a number of novel outcomes including the characterization of magnitude, kinetics, and nature of arteriole remodeling, generation of a working hypothesis of the mechanism governing arteriole remodeling, and elucidation of previously unknown links between LN arteriole remodeling and cellular trafficking, CTL function, and NO regulation, and as such, represent a important step forward in understanding LN physiology and vascularity, arteriole remodeling, and interaction between the microvasculature and immune response.

Figure 21: FITC-Dextran Perfusion Through the Inguinal Lymph Node Feed Arteriole. Inguinal lymph node arteriole (white arrow) and venule (red arrow) following perfusion with 100µl of 1% FITC-dextran in sterile 1x PBS given intra-cardiac and allowed to circulate for ten minutes prior to imaging.

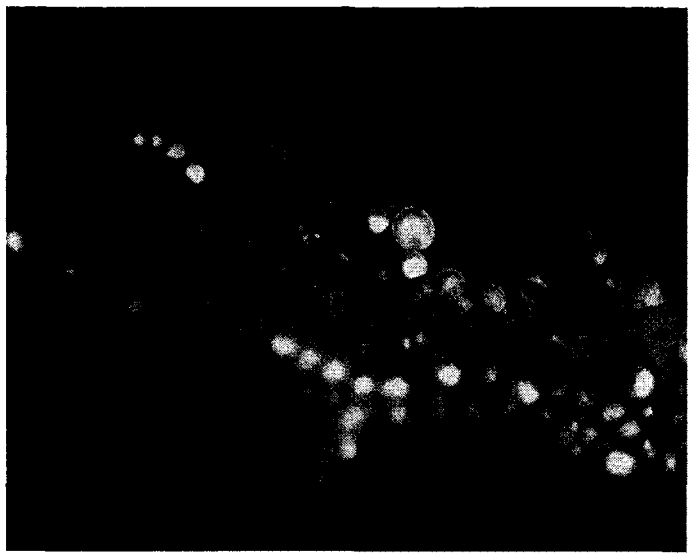

Literature Cited:

Abbas, A.K., K.M Murphy, and A. Sher. 1996. Functional diversity of helper T lymphocytes. *Nature*. 383: 787-93.

Agius, E., *et al.*. 2009. Decreased TNF-alpha synthesis by macrophages restricts cutaneous immunosurveillance by memory CD4+ T cells during aging. *J Exp Med.* 206(9): 1929-40.

Akimitsu, T., D.C. Gute, and R.J. Korthuis. 1995. Leukocyte adhesion induced by inhibition of nitric oxide production in skeletal muscle. *J Appl Physiol.* 78: 1725-32.

Alon, R., and M.L. Dustin. 2007. Force as a facilitator of integrin conformational changes during leukocyte arrest on blood vessels and antigen-presenting cells. *Immunity.* 26(1): 17-27.

Anderson, N.D., A.O. Anderson, and R.G. Wyllie. 1975. Microvascular changes in lymph nodes draining skin allografts. *Amer J Path.* 81(1): 131-153.

Angell, V., *et al.*. 2006. B Cell-Driven Lymphangiogenesis in inflamed lymph nodes enhances dendritic cell mobilization. *Immunity.* 24: 203-215.

Baluk, P., *et al.*. 2009. TNF-alpha drives remodeling of blood vessels and lymphatics in sustained airway inflammation in mice. *J Clinc Invest.* 119(10): 2954-64.

Baker, D.A., and S.A. Plotkin. 1978. Enhancement of vaginal infection in mice by herpes simplex virus type II with progesterone. *Proc Soc Exp Biol Med.* 158: 131–13.

Bajenoff, M., S. Granjeaud, and S. Guerder. 2003. The strategy of T cell antigen-presenting cell encounter in antigen-draining lymph nodes revealed by imaging of initial T cell activation. *J Exp Med.* 198: 715-24.

Behrens, G., *et al.*. 2004. Helper T cells, dendritic cells, and CTL immunity. *Immunol Cell Biol.* 82: 84-90.

Benencia, F., *et al.*. 2003. Nitric oxide and HSV vaginal infection in BALB/c mice. *Virology.* 309: 75-84.

Benest, A.V., *et al.* 2008. Arteriolar genesis and angiogenesis induced by endothelial nitric oxide synthase overexpression results in a mature vasculature. *Arterioscler Throm Vasc Biol.* 28: 1462-68.

Bennett, S.R., *et al.*. 1998. Help for cytotoxic T cell responses is mediated by CD40 signalling. *Nature.* 393: 478-80.

Bousso, P.. 2008. T-cell activation by dendritic cells in the lymph node: lessons from the movies. *Nat Rev Immunol.* 8: 675-84.

Bradley, L.M., *et al.*. 1994. Entry of naïve CD4 T cells into peripheral lymph nodes requires L-selectin. *J Exp Med.* 180: 2401-06.

Bromley, S.K., *et al.*. 2001. The immunological synapse. *Annu Rev Immunol.* 19: 375-96.

Browning, J.L., N. Allaire, A. Ngam-ek, E. Notidis, J. Hunt, S. Perrin, and R.A. Fave. 2005. Lymphotoxin-β receptor signaling is required for the homeostatic control of HEV differentiation and function. *Immunity*. 23: 539-50.

Bucci, M., *et al.*. 2005. Endothelial nitric oxide synthase activation is critical for vascular leakage during acute inflammation *in vivo*. *Proc Natl Acad Sci.* 102(3): 904-8.

Burne, M.J., *et al.*. 2001. Identification of the CD4+ T cell as a major pathogenic factor in ischemic acute renal failure. *J Clinc Invest.* 108(9): 1283-90.

Cameron, DW, JN Simonsen, LJ D'Costa, AR Ronald, GM Maitha, M.N. Gakinya, M Cheang, JO Ndinya-Achola, P Piot, RC Brunham *et al.*. 1989. Female to male transmission of human immunodeficiency virus type 1: risk factors for seroconversion in men. *Lancet.* 2:403-407.

Casrouge, A., *et al.*. 2000. Size estimate of the αβ TCR repertoire of naïve mouse splenocytes. *J Immunol.* 164: 5782-7.

Castellino, F., and R.N. Germain. 2006. Cooperation between CD4+ and CD8+ T cells: When, where, and how. *Annu Rev Immunol.* 24: 519-40.

Cerwinka, W.H., D. Cooper, C.F. Krieglstein, M. Feelisch, and D.N. Granger. 2002. Nitric oxide modulates endotoxin-induced platelet-endothelial cell adhesion in intestinal venules. *Am J Physiol Heart Circ Physiol.* 282: 1111-7.

Chyou, S., *et al.*. 2008. Fibroblast-type reticular stromal cells regulate the lymph node vasculature. *J Immunol.* 181: 3887-96.

Crijns, F.R.L., H.A.J. Struijker Boudier, and B.H.R. Wolffenbuttel. 1998. Arteriolar Reactivity in Concious Diabetic Rats. *Diabetes.* 47: 918-23.

Currica, M.J., *et al.*. 2010. Perivascular T cell infiltration leads to sustained pulmonary artery remodeling after endothelial cell damage. *Am J Respir Cell Mol Biol.*

Dajnowiec, D., and B.L. Langille. 2007. Arterial adaptations to chronic changes in haemodynamic function: coupling vasomotor tone to structural remodelling. *Clinc Sci.* 113: 15-23.

Delay, E., *et al.*. 2008. Pulmonary arterial remodeling induced by a Th2 immune response. *J Exp Med.* 205(2): 361-72.

Ezaki, T. *et al.*. 2001. Time course of endothelial cell proliferation and microvascular remodeling in chronic inflammation. *Am J Pathol.* 158(6): 2043-55.

Ferrara, N., H. Gerber, and J. LeCouter. 2003. The biology of VEGF and its receptors. *Nat Med.* 9(6): 669-76.

Ferrara, N., K. Houck, L. Jakeman, and D.W. Leung. 1992. Molecular and biological properties of the vascular endothelial growth factor family of proteins. *Endocr Rev.* 13(1): 18-32.

Finger, E.B., *et al.*. 1996. Adhesion through L-selectin requires a threshold hydrodynamic shear. *Nature.* 379: 266-269.

Fleming, D.T., G.M. McQuillan, R.E. Johnson, A.J. Nahmias, S.O. Aral, F.K. Lee, and M.E. St. Louis. 1997. Herpes simplex virus type 2 in the United States, 1976 to 1994. *N Engl J Med.* 337: 1105-1111.

Fontana, J., *et al.*. 2002. Domain mapping studies reveal that the M domain of Hsp90 serves as a molecular scaffold to regulate Akt-dependent phosphorylation of endothelial nitric oxide synthase and NO release. *Circ Res.* 90: 866-73.

Frater-Schroder, M., *et al.*. 1987. Tumor necrosis factor type alpha, a potent inhibitor of endothelial cell growth in vitro, is angiogenic in vivo. *Proc Natl Acad Sci.* 84(15): 5277-81.

Freeman, E.E., *et al.*. 2006. Herpes simplex virus 2 infections increases HIV acquisitions in men and women: systematic review and meta-analysis of longitudinal studies. *AIDS.* 20: 73-83.

Germann, W.J., and C.L. Stanfield. *Principles of Human Physiology*. 2nd Edition. Pearson Education Inc., USA, 2005. Pp. 448-86.

Greenberger, N., P. Toskes, and K. Lsselbacher. 1998. *Harrison's Principles of Internal Medicine.* 14th Edition. McGraw-Hill. Chapter 304. Pp 1741-43.

Hall, J.G.. 1974. Observations on the migration and localization of lymphoid cells. *Prog. Immunol.* 11:3-15.

Handsfield, H.H., K.M. Stone, and J.N. Wasserheit.1999. Prevention agenda for genital herpes. *Sex Transm Dis.* 26(4):228–31.

Hatakeyama, T., *et al.*. 2006. Endothelial nitric oxide synthase regulates microvascular hyperpermeability *in vivo*. *J Physiol.* 574.1: 275-81.

Hay, J.B., and B.B. Hobbs. 1977. The flow of blood to lymph nodes and its relation to lymphocyte traffic and the immune response. *J Exp Med.*. 145: 31-44.

Heil, M., *et al.*. 2006. Arteriogenesis versus angiogenesis: similarities and differences. *J Cell Mol Med.* 10(1): 45-55.

Hendriks, H.R., C. Korn, R.E. Mebius, and G. Kraal. 1989. Interferon-gamma-increased adherence of lymphocytes to high endothelial venules. *Immunol.* 68: 221-226.

Hendriks, H.R., A.M. Duijvestijn, and G. Kraal. 1987. Rapid decrease in lymphocyte adherence to high endothelial venules in lymph nodes deprived of afferent lymphatic vessels. *Eur J Immunol.* 17: 1691-95.

Henrickson, S.E., *et al.*. 2008. T cell sensing of antigen dose govern interactive behavior with dendritic cells and sets a threshold for T cell activation. *Nat Immunol.* 9(3): 282-91.

Herman, P.G., I. Yamamoto, and H.Z. Mellins. 1972. Blood microcirculation in the lymph node during the primary immune response. *J Exp Med.*. 136: 697-714.

Hanssen, E.M., *et al.*. 2003. CD4+ T cells are required for secondary expansion and memory in CD8+ T lymphocytes. *Nature.* 421: 852-6.

Jennings, S.R., *et al.*. 1991. CD4-positive T lymphocytes are required for the generation of the primary but not the secondary CD8-positive cytolytic T lymphocyte response to herpes simplex virus in C57 BL/6 mice. *Cell Immunol.* 133(1): 234-52.

Jones, C.A., T.J. Taylor, and D.M. Knipe. 2000. Biological properties of herpes simplex virus 2 replication-defective mutant strains in a murine nasal infection model. *Virology*. 278: 137-50.

Kapsenberg, M.L.. 2003. Dendritic-cell control of pathogen-driven T-cell polarization. *Nat Rev Immunol*. 3: 984-93.

Kaushic, C., A.A. Ashkar, L.A. Reid, and K.L. Rosenthal. 2003. Progesterone increases susceptibility and decreases immune responses to genital herpes infection. *J Virol*. 77: 4558-65.

Koelle, D.M., *et al.*. 1998. Clearance of HSV-2 from recurrent genital lesions correlates with infiltration of HSV-specific cytotoxic T cells. *J Clin Invest*. 101: 1500-08.

Koller, A., and G. Kaley. 1990. Endothelial regulation of wall shear stress and blood flow in skeletal muscle microcirculation. *Am J Physiol Heart Circ Physiol*. 260: H862-68.

Koller, A., and G. Kaley. 1989. Flow velocity-dependent regulation of microvascular resistance in vivo. *Microcirc Endothelium Lymphatics*. 5(6): 519-29.

Kraal, D., K. Schornagel, H. Savelkoul, and T. Maruyama. 1994. Activation of high endothelial venules in peripheral lymph nodes. The involvement of interferon-gamma. *Int Immunol.*. 6: 1195-2101.

Kubes, P., M. Suzuki, and D.N. Granger. 1991. Nitric oxide: an endogenous modulator of leukocyte adhesion. *Proc Natl Acad Sci*. 88: 4651-55.

Kumamoto, Y., L.M. Mattei, S.L. Sellers, G.W. Payne, and A. Iwasaki. 2011. CD4+ T cells support cytotoxic T lymphocyte priming by controlling lymph node input. *Proc Natl Acad Sci*. 108(21): 8749-54.

Kumar, V., *et al.*. 2010. Global lymphoid tissue remodeling during a viral infection is orchestrated by a B cell-lymphotoxin-dependent pathway. *Blood*. 115: 4725-33.

Leibovich, S.J., *et al.*. 1987. Macrophage-induced angiogenesis is mediated by tumour necrosis factor-alpha. *Nature*. 329(6140): 630-2.

Leung, D.W., G. Cachianes, W.J. Kuang, D.V. Goeddel, and N.Ferrara. 1989. Vascular endothelial growth factor is a secreted angiogenic mitogen. *Science*. 246(4935): 1306-9.

Ley, K., *et al.*.2007. Getting to the site of inflammation: the leukocyte adhesion cascade updated. *Nat Rev Immunol*. 7: 678-89.

Li, Y.J. J.H. Haga, and S. Chien. 2005. Molecular basis of the effects of shear stress on vascular endothelial cells. *J Biomech*. 38: 1949-71.

Liao, S., and N.H. Ruddle. 2006. Synchrony of high endothelial venules and lymphatic vessels revealed by immunization. *J Immunol*. 177: 3369-79.

Linton, P.J., and K. Dorshkind. 2004 Age-related changes in lymphocyte development and function. *Nat Immunol*. 8: 133-9.

Lund, J., S. Sato, S. Akira, R. Medzhitov, and A. Iwasaki. 2004. Toll-like receptor 9-mediated recognition of Herpes simplex virus-2 by plasmacytoid dendritic cells. *J Exp Med*. 198(3): 513-20.

Marchesi, V.T., and J.L. Gowans. 1964. The migration of lymphocytes through the endothelium of venules in lymph nodes. An electron microscope study. *Proc R Sco Lond.*159: 238.

Matloubian, M., R.J. Concepcion, and R. Ahmed. 1994. CD4+ T cells required to sustain CD8+ cytotoxic T-cell responses during chronic viral infection. *J Virol.* 68(12): 8056-63.

McDermott, M.R., *et al.*. 1984. Immunity in the Female Genital Tract After Intravaginal Vaccination of Mice with an Attenuted Strain of Herpes Simplex Virus Type 2. *J Virol.* 51(3): 747-53.

McEver, R.P. and C. Zhu. 2007. A catch to integrin activation. *Nat Immunol.* 8: 1035-1037.

McLachlan, J.B., J.P. Hart, S.V. Pizzo, C.P. Shelburne, H.F. Staats, M.D. Gunn, and S.N. Abraham. 2003. Mast cell-derived tumor necrosis factor induces hypertrophy of draining lymph nodes during infection. *Nature Immunology.* **4**(12): 1199-1205.

McLachlan, J.B., C.P. Shelburne, J.P. Hart, S.V. Pizzo, R. Goyal, R. Brooking-Dixon, H.F. Staats, and S.N. Abraham. 2008. Mast cells activators: a new class of highly effective vaccine adjuvants. *Nature Medicine.* **14**(5): 536-541.

Mebius, R.E., *et al.*. 1990. The function of high endothelial venules in mouse lymph nodes simulated by oxazolone. *Immunol.* 71: 423-27.

Medzhitov, R, and D Littman. 2009. HIV immunology needs a new direction. *Nature.* 455: 591.

Metaxa, E., *et al.* 2008. Nitric oxide-dependent stimulation of endothelial cell proliferation by sustained high flow. *Am J Physiol Heart Circ Physiol.* 295: H736-42.

Miyasaka, M., and T. Tanaka. 2004. Lymphocyte trafficking across high endothelial venules: dogmas and enigmas. *Nat Rev Immunol.* 4: 360-70.

Mulvany, M.J.. 1999. Vascular remodelling of resistance vessels: can we define this?. *Cardiovasc Res.* 41: 9-13.

Murohara, T., *et al.*. 1998. Nitric oxide synthase modulates angiogenesis in response to tissue ischemia. *J Clinc Invest.* 101: 2567-78.

Murphy, K. *et al.*. *Janeway's Immunobiology*. Seventh Edition. Garland Science. 2008. Pp. 599-654.

Myking, A.O.. 1980. Morphological changes in paracortical high endothelial venules in single and repeated application of oxazolone to mouse skin. *B Cell Path.* 35: 63-71.

2002. Vascular permeability factor/vascular endothelial growth factor induces lymphangiogenesis as well angiogenesis. *J Exp Med.* 196: 1497-1506.

Nagy, J.A., *et al.*. 2002. Vascular permeability factor/vascular endothelial growth factor induces lymphangiogenesis as well as angiogenesis. *J Exp Med.* 196(11): 1497-506.

Nakanishi, Y., B. Lu, C. Gerard, and A. Iwasaki. 2009. CTL mobilization to virus-infected tissue requires CD4+ T cell help. *Nature.* 462(7272): 510-513.

Nieves, B.J., P.A. D'Amore, and B.A. Bryan. 2009. The function of vascular endothelial growth factor. *Biofactors.* 35(4): 332-7.

Norman, M.U., L. Zbytnuik, and P.Kubes. 2008. Interferon-gamma limits Th1 lymphocyte adhesion to inflamed endothelium: a nitric oxide regulatory feedback mechanism. *Eur J Immunol.* 38: 1368-80.

Obar, J.J., K.M. Khanna, and L. Lefrancois. 2008. Endogenous naïve CD8+ T cell precursor frequency regulates primary and memory responses to infection. *Immunity.* 28: 859-69.

Obarr, J.J., *et al.*. 2010. CD4+ T cell regulation of CD25 expression controls development of short-lvied effector CD8+ T cells in primary and secondary responses. *Proc Natl Acad Sci USA.* 107: 193-98.

Overall, J.C. Jr., *et al.*. 1975. Genital herpesvirus hominis infection in mice. I. Development of an experimental model. *Infect Immun.* 11(3): 476-80.

Palframan, R.T., *et al.*. 2001. Inflammatory chemokine transport and presentation in HEV: a remote control mechanism for monocyte recruitment to lymph nodes in inflamed tissues. *J Exp Med.* 194(4): 1361-73.

Papapetropoulos, A., G. Garcia-Cardena, J.A. Madri, and W.C. Sessa. 1997. Nitric oxide production contributes to the angiogenic properties of vascular endothelial growth factor in human endothelial cells. *J Clinc Invest.* 100: 3131-39.

Parr, M.B., *et al.* 1994. A mouse model for studies of mucosal immunity to vaginal infection by herpes simplex virus type 2. *Lab Invest.* 70(3): 369-80.

Polverini, P.J., R.S. Cotran, and M.M. Sholley. 1977. Endothelial proliferation in the delayed hypersensitivity reaction: an autoradiographic study. *J Immunol.* 118: 277-96.

Pries, A.R., and T.W. Secomb. 2002. Structural adaptation of microvascular networks and development of hypertension. *Microcirc.* 9: 305-14.

Puddell, A.P., *et al.*. 2003. B lymphocyte-specific c-Myc expression stiulates early and function expansion of the vasculature and lymphatics during lymphomagenesis. *Am J Pathol.* 163: 2233-45.

Rajasagi, N.K., *et al.*. 2009. CD4+ T cells are required for the priming of CD8+ T cells following infection with herpes simplex virus type 1. *J Virol.* 8: 5256-68.

Randolph, G.J., V. Angeli, and M.A. Swartz. 2005. Dendritic-cell trafficking to lymph nodes through lymphatic vessels. *Nat Rev Immunol.* 5: 617-28.

Sato, A., M.M. Linehan, and A. Iwasaki. 2006. Dual recognition of herpes simplex viruses by TLR2 and TLR9 in dendritic cells. *Proc Natl Acad Sci.* 103(46): 17343-48.

Ridger, V., Krams, R., Carpi, A. and P.C. Evans. 2008. Hemodynamic parameters regulating vascular inflammation and atherosclerosis: a brief update. *Biomed Pharmacother.* 62: 536-540.

Sellers, S.L., and G.W. Payne. 2011. Intravital microscopy of the inguinal lymph node. *J Vis Exp.*

Sessa, W.C.. 2009. Molecular control of blood flow and angiogenesis: role of nitric

oxide. *J Thromb Haemost.* 7(1): 35-7.

Sessa, W.C.. 2004. eNOS at a glance. *J. Cell Sci.*. 117: 2427-2429.

Shrestha, B., *et al.*. 2010. B Cell-Derived Vascular Endothelial Growth Factor A Promotes Lymphangiogenesis and High Endothelial Venule Expansion in Lymph Nodes. *J Immunol.* 184: 4819-26.

Sidky, Y.A., and R. Auerbach. 1975. Lymphocyte-induced angiogenesis: a quantitative and sensitive assay of the graft-vs.-host reaction. *J Exp Med.* 141: 1084-1100.

Smith, C.M., *et al.*. 2004. Cognate CD4+ T cell licensing of dendritic cells in CD8+ T cell immunity. *Nat Immunol.* 5: 1143-48.

Soderberg, K.A., *et al.*. 2005. Innate control of adaptive immunity via remodeling of lymph node feed arteriole. *Proc Natl Acad Sci.* 102(45): 16315-20.

Stabile, E., *et al.*. 2003. Impaired arteriogenic response to acute hindlimb ischemia in CD4-knockout mice. *Circ.* 108: 205-10.

Stamm, WE, HH Handsfield, AM Rompalo, RL Ashley, PL Roberts, and L Corey. 1988. The association between genital ulcer disease and acquisition of HIV infection in homosexual men. *Jama.* 260: 1429-1433.

Stuttfeld, E., and K. Ballmer-Hofer. 2009. Structure and function of VEGF receptors. *Life.* 61(9): 915-22.

Sucosky, P., Balachandran, K., Elhammali, A., Jo, H. and A.P. Yoganathan. 2009. Altered shear stress stimulates upregulation of endothelial VCAM-1 and ICAM-1 in a BMP-4- and TGF-beta1-dependent pathway. *Arterioscler Thromb Vasc Biol.* 29: 254-260.

Sundrani, R., *et al.*. 2000. Nitric oxide synthase inhibition increases venular leukocyte rolling and adhesion in septic rats. *Crit Care Med.* 28(8): 2898-2903.

Takedachi, M., *et al.*. 2008. CD73-generated adenosine restricts lymphocyte migration into draining lymph nodes. *J Immunol.* 180: 6288-96.

Vallejo, A.N.. 2007. Immune remodeling: lessons from repertoire alterations during chronological aging and in immune-mediated disease. *Trends Mol Med.* 13(3): 94-102.

Vanhoutte, P.M.. 2003. Enothelial Control of Vasomotor Function. *Circ J.* 67: 572-75.

Villadangos, J.A., and P. Schnorrer. 2007. Intrinsic and cooperative antigen-presenting functions of dendritic-cell subsets *in vivo*. *Nat Rev Immunol.* 7: 543-55.

Von Andrian, U.H., and T.R. Mempel. 2003. Homing and cellular traffic in lymph nodes. *Nat Rev Immunol.* 3: 867-78.

Webster, B., *et al.*. 2006. Regulation of lymph node vascular growth by dendritic cells. *J Exp Med.* 203(8): 1903-13.

Wozniak, K.L., M.L. Young, and F.L. Wormley Jr.. 2011. Protective Immunity against experimental pulmonary cryptococcosis in T cell-depleted mice. *Clin Vaccine Immunol.* 18(5): 717-23.

Yu, J. *et al.*. 2005. Endothelial nitric oxide synthase is critical for ischemic remodeling, mural cell recruitment, and blood flow reserve. *Proc Natl Acad Sci.*. 102(31): 10999-11004.

Zhao, W.L., *et al.*. 2004. Vascular endothelial growth factor-A is expressed both on lymphoma cells and endothelial cells in angioimmunoblastic T cell lymphoma and related to lymphoma progression. *Lab Invest.* 84: 1512-19.

Zhu, J., *et al.*. 2009. Persistence of HIV-2 receptor-positive cells after HSV-2 reactivation is a potential mechanism for increased HIV-1 acquisition. *Nat Med.* 15(8): 886-93.

Zwacka, R.M., *et al.*. 1997. CD4(+) T-lymphocytes mediate ischemia/reperfusion injury in mice. *Am J Physiol.*. 279: F525-31.